Cell Stem Cell

Clinical and Translational Report

Genomic and transcriptomic quality control for an autologous iPSC-derived cell therapy for Parkinson's disease

Graphical abstract

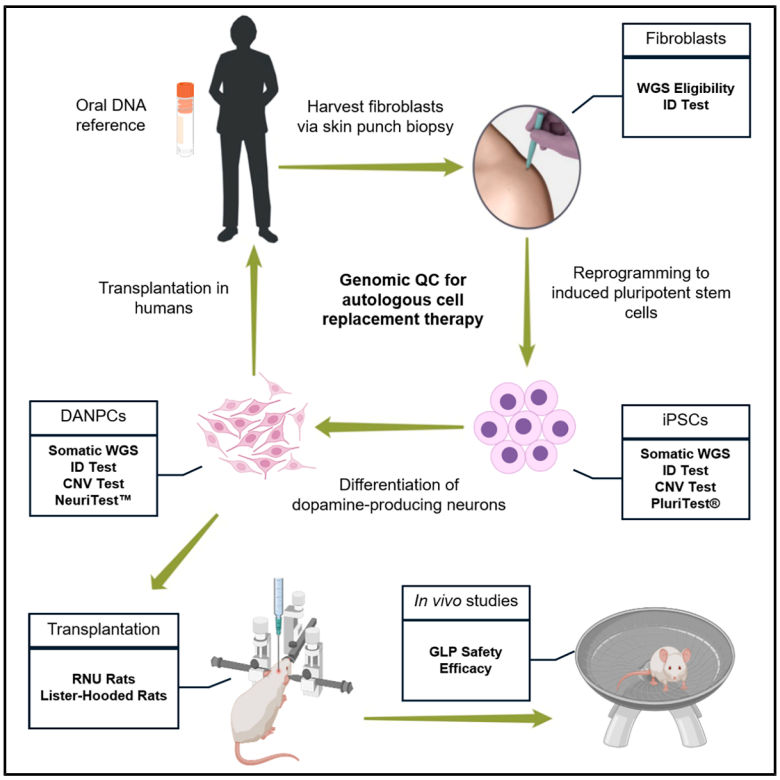

Highlights

- Reproducible genomic and transcriptomic qualification of DANPCs across multiple donors
- DANPCs reversed motor dysfunction in 6-OHDA-lesioned Parkinsonian rats
- DANPCs exhibited no adverse effects in a 9-month GLP safety study
- An autologous phase 1/2a clinical trial to treat PD patients is ongoing

Authors

Andres M. Bratt-Leal, Thorsten Gorba, Roy M. Williams, ..., Jeanne F. Loring, Edward D. Wirth III, Xiaokui Zhang

Correspondence

abrattleal@aspenneuro.com

In brief

Bratt-Leal et al. report the preclinical data supporting initiation of a clinical trial investigating autologous dopaminergic neuron precursor cell therapy for moderate to advanced Parkinson's disease patients. Whole-genome sequencing and RNA-seq analysis underpin a quality control program to ensure safety and efficacy.

Bratt-Leal et al., 2026, Cell Stem Cell *33*, 1–15
October 1, 2026 © 2026 The Authors. Published by Elsevier Inc.
https://doi.org/10.1016/j.stem.2026.08.014

CellPress

Please cite this article in press as: Bratt-Leal et al., Genomic and transcriptomic quality control for an autologous iPSC-derived cell therapy for Parkinson's disease, Cell Stem Cell (2026), https://doi.org/10.1016/j.stem.2026.08.014

Cell Stem Cell

CellPress
OPEN ACCESS

Clinical and Translational Report

Genomic and transcriptomic quality control for an autologous iPSC-derived cell therapy for Parkinson's disease

Andres M. Bratt-Leal,[1,8,*] Thorsten Gorba,[1,4] Roy M. Williams,[1,4] Jim A. Mossman,[1,4] Rachel Hills,[2,4] Ha Tran,[1] Derren Barken,[1] Genevieve Beauvais,[1] Daniel Fremgen,[1] Ai Zhang,[1,5] Cullen Pivaroff,[1] Candace Lynch,[1] Yanzheng Liu,[1] Chandnee Chandrasekaran,[1] David Tastad,[1] Charlotte Bridge,[2] Dustin R. Wakeman,[1,6] Uyen Nguyen,[1] Brent Chamberlain,[1,7] Emma L. Lane,[2] Mariah J. Lelos,[2] Jeanne F. Loring,[3] Edward D. Wirth III,[1] and Xiaokui Zhang[1]
[1]Aspen Neuroscience, San Diego, CA, USA
[2]Brain Repair Group, School of Biosciences, Cardiff University, Cardiff, UK
[3]Scripps Research Institute, La Jolla, CA, USA
[4]These authors contributed equally
[5]Present address: Genentech, San Francisco, CA, USA
[6]Present address: Omixell, San Diego, CA, USA
[7]Present address: Jefferson Institute for Bioprocessing, Philadelphia, PA, USA
[8]Lead contact
*Correspondence: abrattleal@aspenneuro.com
https://doi.org/10.1016/j.stem.2026.08.014

SUMMARY

Toward development of an autologous, induced pluripotent stem cell (iPSC)-based cell therapy for Parkinson's disease (PD), we demonstrate successful, reproducible genomic and transcriptomic qualification of patient-derived dopaminergic neuron precursor cells (DANPCs) across multiple donors. Our analysis includes whole-genome sequencing data from fibroblasts, iPSCs, and DANPCs and the development of NeuriTest, an RNAseq-based bioinformatic analysis of DANPCs designed to predict cell quality based on empirical animal data. Autologous cell therapies are immune matched to the patient, potentially augmenting durability of benefit compared to allogeneic cells while negating the need for immunosuppression and accompanying side effects. Patient-specific iPSCs are an autologous cell source that can be differentiated to dopaminergic neurons, the cell type lost in PD. We report here our preclinical manufacturing strategy and results demonstrating efficacy in a PD rodent model and safety in a 9-month GLP toxicology study.

INTRODUCTION

Parkinson's disease (PD) is a progressive neurodegenerative disorder marked by the selective loss of dopaminergic neurons in the midbrain, leading to hallmark motor symptoms such as tremor, rigidity, bradykinesia, and postural instability. While current dopamine (DA)-based pharmacological therapies temporarily alleviate symptoms, they neither prevent ongoing neurodegeneration nor restore lost neurons. Cell replacement therapy, aimed at repopulating dopaminergic neurons, offers a promising disease-modifying strategy. Studies of cell transplants in animal models suggest that transplanted dopaminergic cells may do more than just produce DA; they can also provide innervation to striatal and extrastriatal DA targets and partially recreate proper neural networks with synaptic DA release.[1]

Early clinical attempts to replace lost dopaminergic neurons using fetal midbrain tissue yielded variable outcomes, but a small number of patients experienced sustained clinical benefit.[2–4] The variability in tissue quality, difficulty sourcing tissue, and ethical constraints associated with fetal tissue led to the exploration of human pluripotent stem cells (hPSCs), including embryonic stem cells (hESCs) and induced pluripotent stem cells (iPSCs), as a more scalable and controlled source of dopaminergic neurons. Multiple differentiation protocols have been developed to reproducibly yield midbrain dopaminergic precursors from hPSCs that have demonstrated efficacy in animal models.[5–12]

Three first-in-human trials using allogeneic hESC- or iPSC-derived dopaminergic precursors have recently reported encouraging outcomes, showing acceptable safety profiles and signs of clinical improvement within the first 2 years post transplantation.[13–15] However, allogeneic approaches require immunosuppression, which carries risks such as opportunistic infection, malignancy, systemic toxicity, and death.[13,14,16]

In contrast, dopaminergic neurons derived from autologous iPSCs are not likely to require immunosuppression, since patients receive their own cells. Results from a nonhuman primate

This is an open access article under the CC BY license (http://creativecommons.org/licenses/by/4.0/).

Please cite this article in press as: Bratt-Leal et al., Genomic and transcriptomic quality control for an autologous iPSC-derived cell therapy for Parkinson's disease, Cell Stem Cell (2026), https://doi.org/10.1016/j.stem.2026.08.014

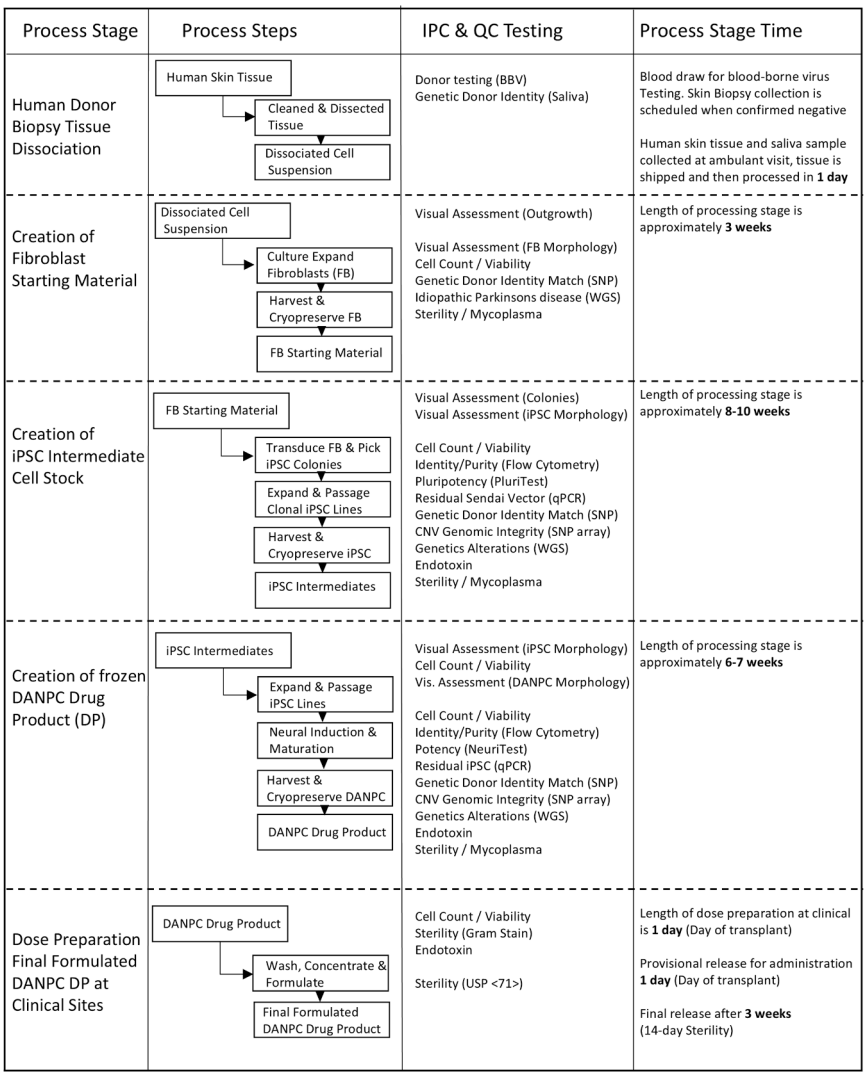

Figure 1. Process workflow schematic for manufacturing under GMP

Process flow diagram and workflow table summarizing the main unit operations, analytics for in-process-control (IPC) and QC release testing, and process durations for the sequential DANPC cell product manufacturing process stages (skin to brain). For the creation of fibroblast, iPSC and DANPC material-generation process stages in the testing column, the in-process testing is listed first, with the QC release testing for further manufacturing and drug product disposition shown underneath the gap. The release criteria for the iPSC intermediate and the DANPC drug product are described in Table 1. For the fibroblast starting material, the release criteria for further manufacturing are sterility and mycoplasma (pass), donor identity matches saliva donor reference (pass), absence of familial PD driver mutations (pass), visual assessment of fibroblast morphology (pass) and viability (report results). See also Table S1.

(NHP) model of PD revealed more thorough and effective integration of autologous iPSC-derived dopaminergic precursors transplanted into the brain compared with transplants of cells derived from allogeneic iPSCs without immunosuppression.[17] Others have also demonstrated recovery in NHP models of PD using autologous cells without immunosuppression.[18,19] A single-patient (N = 1) study reported up to 24-month outcomes following transplantation of autologous iPSC-derived cells without immunosuppression, supported by corresponding preclinical data.[20] However, these preclinical studies were limited to cells derived from the same individual, constraining assessment of inter-donor reproducibility. Extending this approach to multi-patient autologous trials will require robust demonstration of reproducibility and quality control (QC) across donors to enable clinical development of patient-specific cell products without individualized preclinical testing.

In this study, we present preclinical data and our manufacturing strategy (Figure 1) for developing an autologous iPSC-derived dopaminergic precursor cell (DANPC) therapy for PD. Our approach addresses safety concerns by implementing whole-genome sequencing (WGS) at multiple stages of iPSC derivation and differentiation. To address the challenge of reproducibly qualifying individual cultures of DANPCs for optimal efficacy,[8] we used machine learning (ML) to develop a transcriptomic assay "NeuriTest" building on the PluriTest model.[21] NeuriTest quantifies the similarity of a transcriptome to profiles that correlate with preclinical efficacy and guides refinements to the research-grade differentiation process[7] to a clinical-grade differentiation process that produced similarly efficacious cells. In contrast to scale-up processes used for allogeneic products, we employ a cost-effective fail-fast manufacturing paradigm that identifies quality control failures early in the process. The data reported served as the foundation for the investigational new drug (IND) application reviewed by the Food and Drug Agency and the launch of the Autologous-derived Study of a Parkinson's Investigational Regenerative therapy in an Open label trial (ASPIRO), the first multicenter phase 1/2a clinical trial of autologous iPSC-derived dopaminergic neuron replacement for PD (ClinicalTrials.gov ID: NCT06344026). Dosing of the first two patient cohorts was completed in 2024. Here, we describe the scientific rationale, preclinical data, and QC metrics we developed to support this personalized therapeutic approach.

RESULTS

Unlike an allogeneic approach that requires qualification of a master cell bank and a working cell bank for a single-cell line, autologous cell product generation requires extensive quality control testing for each patient-specific cell line at intermediate stages during manufacturing and at product release using pass-fail criteria established in advance. We report results of standard attribute (conventional) quality control methods and

Please cite this article in press as: Bratt-Leal et al., Genomic and transcriptomic quality control for an autologous iPSC-derived cell therapy for Parkinson's disease, Cell Stem Cell (2026), https://doi.org/10.1016/j.stem.2026.08.014

Table 1. Quality control assays

Test	Method	Release criterion	Cell-line lot						
			109_Sa03	109_Sa12	425_Sa02b	425_Sa13a	425_Sa15a	457_Sa05	457_Sa18
Standard attribute quality control assays: undifferentiated iPSCs									
Sterility	United States Pharmacopeia (USP) <71>	negative for growth	pass	pass	pass	pass	pass	pass	pass
Mycoplasma	qRT-PCR	not detected	pass	pass	pass	pass	pass	pass	pass
Endotoxin	limulus amebocyte lysate (LAL)	≤5 EU/mL	0.045	0.032	0.031	<0.050	<0.050	<0.050	<0.050
Post-thaw viability	NucleoCounter	≥80%	99.5%	99.5%	99.7%	99.4%	99.5%	99.0%	99.2%
Identity	flow cytometry	OCT3/4+ > 80%; TRA-1-81+ > 80%	OCT3/4+: 91.2%; TRA-1-81+: 92.1%	OCT3/4+: 93.8%; TRA-1-81+: 95.2%	OCT3/4+: 98.3%; TRA-1-81+: 95.3%	OCT3/4+: 97.4%; TRA-1-81+: 95.9%	OCT3/4+: 93.7%; TRA-1-81+: 87.8%	OCT3/4+: 94.8%; TRA-1-81+: 94.1%	OCT3/4+: 93.9%; TRA-1-81+: 97.6%
Residual Sendai virus	qRT-PCR	<5 copies/100 cells	<0.2	<0.3	<0.3	3.9	<0.3	<0.2	<0.3
Standard attribute quality control assays: DANPCs									
Sterility	USP <71>	negative for growth	pass	pass	pass	pass	pass	pass	pass
Mycoplasma	qRT-PCR	not detected	pass	pass	pass	pass	pass	pass	pass
Endotoxin	LAL	≤1.0 EU/mL	0.055	<0.050	<0.050	<0.050	<0.050	<0.050	0.058
Post-thaw viability	NucleoCounter	≥80% viable	81.9%	89.2%	90.5%	89.7%	90.5%	93.3%	92.1%
Identity	flow cytometry	FOXA2+ > 80%	97.5%	98.3%	98.7%	99.4%	99.4%	90.9%	91.7%
Identity	flow cytometry	OTX2+ (no release criteria)	90.1%	68.3%	95.5%	86.3%	85.4%	89.5%	95.5%
Impurity (multipotent neural progenitors)	flow cytometry	PAX6+ < 5%	0.1%	0.6%	0.1%	0.2%	0.9%	4.7%	3.3%
Residual pluripotent cells	qRT-PCR	POU5F1 < 0.1%, VRTN < 0.1%	pass	pass	pass	pass	pass	pass	pass
Genomic assays specific for autologous cell therapy: undifferentiated iPSCs									
Genomic structural integrity (CNV)	SNP array	no CNV > 30 Mbp present	pass	pass	pass	pass	pass	pass	pass
Genomic assessment for oncogenic gene mutations	WGS (NCI Genomic Data Commons)	no oncogenic mutations	not detected	not detected	not detected	not detected	not detected	not detected	not detected

(*Continued on next page*)

CellPress
OPEN ACCESS

Please cite this article in press as: Bratt-Leal et al., Genomic and transcriptomic quality control for an autologous iPSC-derived cell therapy for Parkinson's disease, Cell Stem Cell (2026), https://doi.org/10.1016/j.stem.2026.08.014

Table 1. *Continued*

Test	Method	Release criterion	Cell-line lot							
			109_Sa03	109_Sa12	425_Sa02b	425_Sa13a	425_Sa15a	457_Sa05	457_Sa18
PluriTest	RNA-seq	predict pluripotency	pass	pass	pass	pass	pass	pass	pass
Genomic assays specific for autologous cell therapy: DANPCs									
Identity of donor	SNP genotype	$R^2 \geq 0.98$	0.99	0.98	0.99	0.98	0.98	0.99	0.98
Genomic structural integrity (CNV)	SNP array	no CNV > 30 Mbp present	pass	pass	pass	pass	pass	pass	pass
Genomic assessment for oncogenic gene mutations	WGS (NCI Genomic Data Commons)	no oncogene mutations detected	not detected	not detected	not detected	not detected	not detected	not detected	not detected
NeuriTest	RNA-seq	predict DA neuronal differentiation	NeuriScore7.4, novelty score: 0.10	NeuriScore6.4, novelty score: 0.11	NeuriScore8.1, novelty score: 0.10	NeuriScore6.4, novelty score: 0.11	NeuriScore6.9, novelty score: 0.11	NeuriScore2.2, novelty score: 0.07	NeuriScore 3.6, novelty score: 0.06

of genomics-based assays that we developed to ensure genomic integrity and appropriate phenotype.

iPSCs were generated by reprogramming fibroblasts collected under an approved protocol (Scripps Research IRB-HSC-08-5109) from skin biopsies of subjects with moderate PD. The fibroblasts were reprogrammed using nonintegrating Sendai virus (CTS Cytotune-iPSC 2.1, ThermoFisher Scientific). iPSC colonies were identified by morphology and selected for subculture. Culture medium was exchanged daily and the cells were passaged when reaching confluency of 60% or greater. The iPSCs were harvested and cryopreserved at passage 10, and at least 2 iPSC clones were selected from each individual and analyzed by quality control criteria. The results reported here encompass iPSC clones from six individuals with PD (Table S1).

DANPCs were differentiated from the iPSCs using modifications of published protocols.[5,9,13,14,22,23] Briefly, the iPSCs were neuralized using dual SMAD inhibition,[24] regionalized toward midbrain floorplate, and then cultured with neurotrophic factors to promote a dopaminergic neuron fate.[7]

Standard attribute quality control assessment of iPSCs and DANPCs

The cell lots used in the efficacy and safety studies were released with certificates of analyses (CoAs) comprising the set of standard attribute QC and genomic QC assays (Table S2). Seven clones from 3 subjects were used for the pilot manufacturing runs; results are shown in Table 1. Sterility testing verified that the cultures were free of mycoplasma and other bacterial contamination, and they were endotoxin negative. Viability after thawing was confirmed to be greater than 80%. Flow cytometry using antibodies to pluripotency-associated markers (OCT3/4 and TRA-1-81) was used to qualify the identity of the cells as iPSCs, with a passing threshold of >80% of the cells testing positive. Clearance of the Sendai reprogramming vector was confirmed by quantitative RT-PCR (qRT-PCR).

Following differentiation to the appropriate stage of neural development, DANPCs were cryopreserved and characterized using the quality control release criteria (Table 1). DANPCs were tested for sterility, mycoplasma, endotoxin, and viability post-thaw, with all lots passing release criteria. Cell identity was assessed by flow cytometry using antibodies to the transcription factor Forkhead box protein A2 (FOXA2), with a pass level of >80%, as well as the transcription factor orthodenticle homeobox 2 (OTX2). To test for the absence of multipotent neural progenitors, the transcription factor paired box 6 (PAX6) was measured by flow cytometry, to ensure less than 5% expression in the cell preparations. To detect residual undifferentiated iPSCs, qRT-PCR was performed to detect expression of pluripotent stem cell-associated genes Pit1/Oct2/unc-86 (POU) class 5 homeobox 1 (*POU5F1*) and vertebrae development-associated gene (*VRTN*, also known as C14orf115).[25] When compared with controls containing spiked-in undifferentiated iPSCs, the proportion of undifferentiated cells was calculated to be <0.1% (Figure S1A). To ensure the qRT-PCR conditions were sufficient for detection of undifferentiated cells, we used a sensitive *in vitro* assay[26] for detection of contamination with undifferentiated cells.

Please cite this article in press as: Bratt-Leal et al., Genomic and transcriptomic quality control for an autologous iPSC-derived cell therapy for Parkinson's disease, Cell Stem Cell (2026), https://doi.org/10.1016/j.stem.2026.08.014

CellPress
OPEN ACCESS

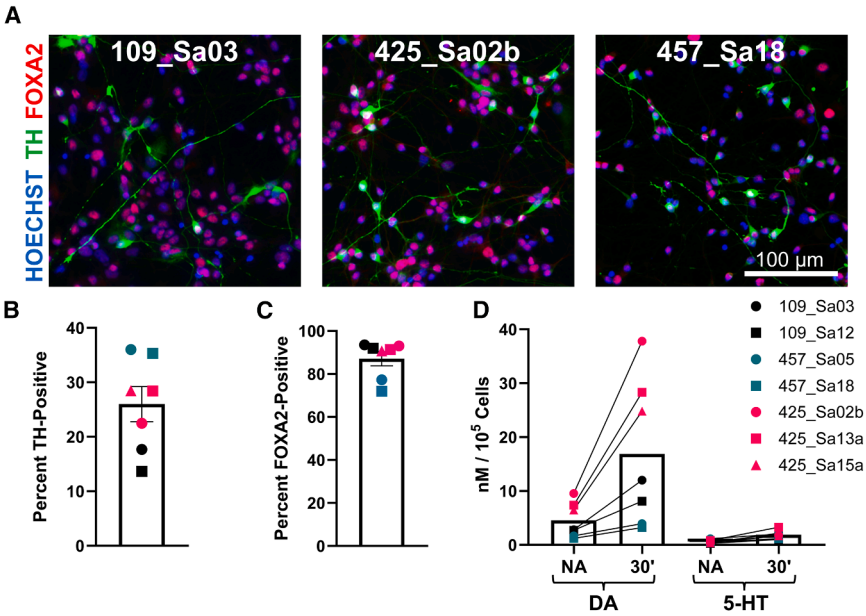

Figure 2. Immunocytochemistry and neurotransmitter release

(A) Representative images of further differentiation of DANPCs at day 32. Immunocytochemistry performed with antibodies against FOXA2 (red) and TH (green). Nuclei stained with Hoescht (blue).
(B) Quantification of TH^+ cells for each DANPC lot.
(C) Quantification of $FOXA2^+$ cells for each DANPC lot.
(D) Quantification of the neurotransmitters dopamine (DA) and serotonin (5-HT) released from unstimulated (NA) or stimulated (30′) DANPCs matured for 60 days after differentiation (nM, normalized to 10^5 cells).
Scale bar: 100 µm (A). Data are represented as mean ± SEM (B and C).
See also Figure S2 and Table S1.

Cultures of DANPCs were spiked with undifferentiated iPSCs at 10%, 1%, 0.05%, and 0.01%, and cultured in iPSC growth medium for 4 days. Colonies of iPSCs arose in cultures with all concentrations of spiked cells, while no colonies emerged in cultures of DANPCs without added undifferentiated cells (Figure S1B).

Functional confirmation of on-target dopaminergic lineage cell fate

DANPCs were matured *in vitro* to assess their purity and functional potential after maturation. After 12 days of maturation, immunocytochemistry analysis demonstrated that tyrosine hydroxylase (TH) was expressed in an average of 26.0% of the cells (Figures 2A and 2B), and FOXA2 was expressed in an average of 87.1% of the cells (Figures 2A and 2C). To assess differentiated neuronal function, DANPCs were matured for a further 60 days and stimulated with potassium chloride (KCl) to measure release of DA and serotonin (5-hydroxtryptamine [5-HT]). All matured DANPCs released neurotransmitters in response to stimulation, at an average of 16.9 nM DA per 100,000 cells and an average of 1.9 nM 5-HT per 100,000 cells (Figure 2D). Given that noradrenergic neurons can also synthesize and release DA, RNA-seq analysis confirmed the absence of noradrenergic gene expression in mature cultures (Figure S1C). Genes associated with mesoderm, endoderm, and neural crest were either not detected or expressed at very low levels (Figure S2).

Genomics-based quality control assays designed for autologous cell therapy

We developed a comprehensive, multi-step bioinformatics pipeline to monitor genomic characteristics associated with the donor identity, efficacy, and safety of autologous cellular derivatives. This pipeline includes multiple methods, each designed to address specific aspects of the therapeutic development process (Table 1; Figure 3).

Donor identity

Single-nucleotide polymorphism (SNP) microarray genotyping of oral swabs obtained at the time of skin biopsy was matched to cultures of skin fibroblasts, iPSCs, and DANPCs across manufacturing stages. Identity was confirmed using an 81-SNP panel with a stringent threshold of B-allele frequency (BAF) least-squares regression coefficient of determination $R^2 \geq 0.98$ (Figure 3A).

Germline and somatic mutation analyses

WGS was performed to assess both inherited and culture-acquired genomic variants. Germline analysis identifies disease-associated mutations or variants inherent to the donor. Donor fibroblasts derived from the skin biopsy were analyzed by WGS to exclude familial pathogenic or likely pathogenic PD mutations by comparing to the human reference genome (Figure 3B; Table S3; https://www.ncbi.nlm.nih.gov/clinvar/). The cell lines reported here were free of PD-related germline mutations (Table 1).

Pluripotent stem cells are known to acquire genomic mutations and structural changes as they are expanded in cell culture, and those aberrations can become dominant in cultures by positive selection.[27–30] Because each autologous iPSC line is expanded only to generate product for a single patient, the risk of mutation acquisition and accumulation is inherently lower than in large-scale allogeneic production.[30,31] To detect *de novo* somatic mutations arising during manufacturing, we conducted somatic variant analyses by comparing iPSC and DANPC genome sequences to their donor-specific fibroblast reference sequences. The somatic test is similar to the tumor-normal pair comparison approach used in cancer genomics[32] and serves as a proactive monitoring strategy to mitigate risks associated with genetic alterations. WGS identified no mutations with established clinical significance, including oncogenic variants in a curated database (NCI Genomic Data Commons; https://portal.gdc.cancer.gov/) (Tables 1 and S4; Figure 3B).[32] All cell lines reported here passed this test (Tables 1 and S4).

Copy-number variant screening for genomic integrity

Genome-wide copy-number variant (CNV) analysis was performed for all samples as part of routine genomic quality control.

Please cite this article in press as: Bratt-Leal et al., Genomic and transcriptomic quality control for an autologous iPSC-derived cell therapy for Parkinson's disease, Cell Stem Cell (2026), https://doi.org/10.1016/j.stem.2026.08.014

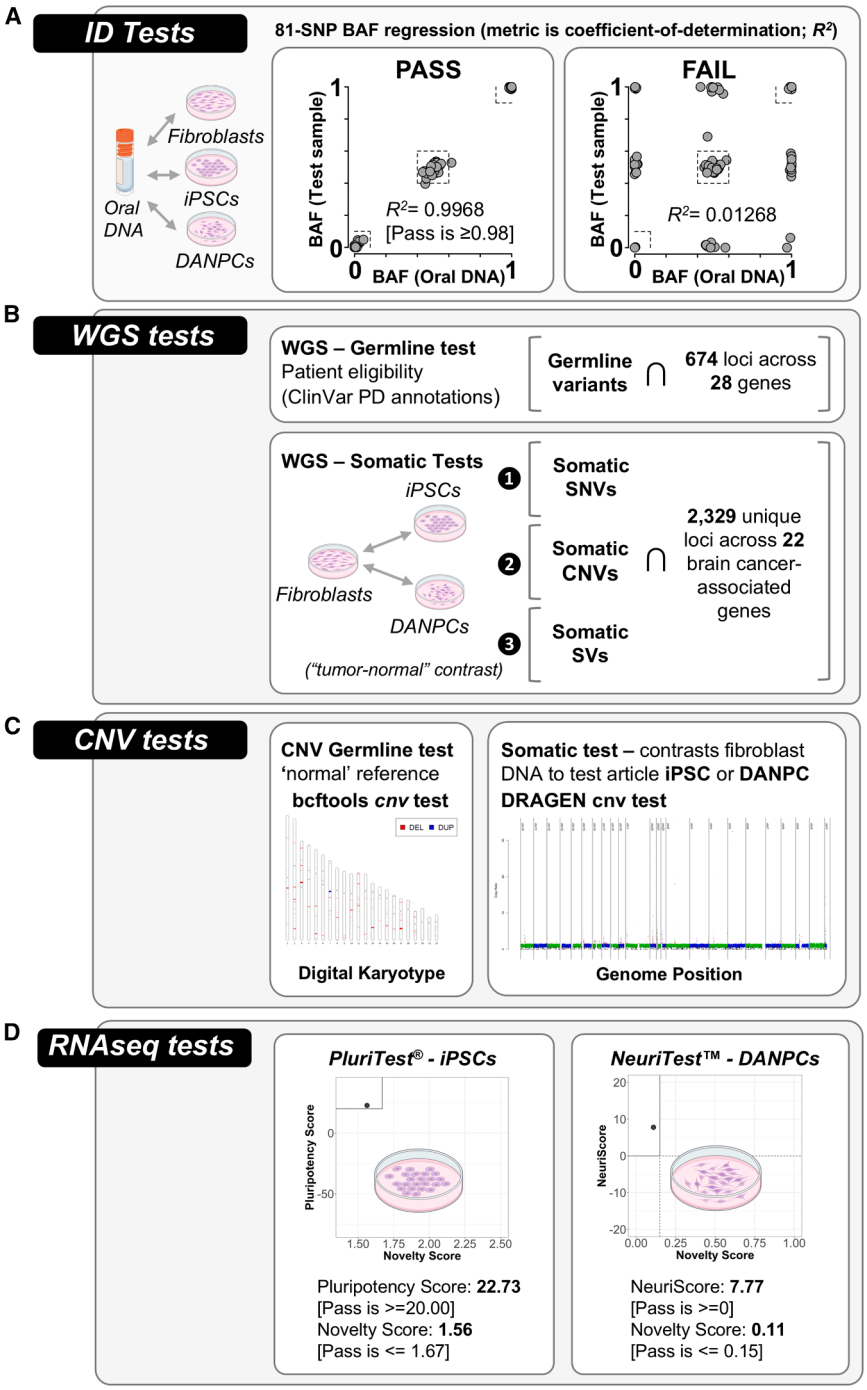

Figure 3. Bioinformatic interrogation of process intermediates and drug substance

(A) Identity test: DNA SNP array of oral DNA. The oral SNP data are used to ensure that the cells match the donor at each stage of the manufacturing process. The B-allele frequencies (BAFs) of 81 highly-discriminating SNPs were compared between the oral DNA reference for the individual (fibroblast, iPSCs, or DANPCs). Least-squares regressions with a coefficient of determination (R^2) $\geq$ 0.98 are genetic matches with identical genotypes at all loci. Any single genotype mismatch caused the regression to drop below the cutoff and was considered a FAIL.

(B) Whole-genome sequencing (WGS) of fibroblasts, iPSCs, and DANPCs. The fibroblast sequence was analyzed for familial PD variants that would exclude the donor from the eligibility for the clinical trial. The fibroblast sequence served as a reference to detect somatic variants that may have accrued at iPSC and DANPC stages. Somatic variants were examined for overlap with known brain cancer-associated mutations. Single-nucleotide variants (SNVs), copy-number variants (CNVs), and structural variants (SVs) in the somatic variant call format (.vcf) output file were intersected with the cancer-associated mutations, and the cell line was disqualified if an intersecting mutation was detected.

(C) Copy-number variants (CNVs) were prescreened on SNP arrays to identify large CNVs before WGS was performed; samples that passed the SNP array assay were tested for somatic CNVs using WGS data.

(D) Two RNA-seq-based machine learning (ML) models were used to test for transcriptome features consistent with known iPSC and DANPC identities: PluriTest and NeuriTest, respectively. Novelty score, pluripotency score, and NeuriScores consistent with target cell types have been established to guide selection of clones for further manufacture and clinical use. All values presented are for illustrative purposes only and not derived from experimental results.

See also Figures S3 and S4 and Tables S1, S3, S4, and S5.

Structural integrity of the genome of the iPSCs and DANPCs was monitored by CNV screening for deletions, duplications, and loss of heterozygosity (Figure 3C).[33] QC failure was defined by exceeding predefined thresholds for overall CNV burden or chromosome-level CNV accumulation. CNVs were detected in all samples, as reflected by the summed autosomal CNV burden (Table S5). Large deletions or duplications (>30 megabase pairs [Mbp]) would exclude a sample from further processing. All seven of the cell lots used for manufacturing passed CNV QC (Table 1; Figure S3).

Application of the same CNV QC pipeline to a broader internal dataset of more than 500 samples resulted in a CNV QC failure rate of approximately 14%, typically driven by large cumulative CNV burden or extensive chromosome-level alterations (Table S5).

Pluripotency assay: PluriTest

Prior to differentiation into DANPCs, donor iPSCs were evaluated with PluriTest, a transcriptome-based assay that replaces *in vivo* (teratoma) and *in vitro* (embryoid body) pluripotency methods,[21] that have been used widely to confirm pluripotency of human cells.[34,35] All tested lines passed both the pluripotency (similarity to confirmed pluripotent cells) and novelty

Please cite this article in press as: Bratt-Leal et al., Genomic and transcriptomic quality control for an autologous iPSC-derived cell therapy for Parkinson's disease, Cell Stem Cell (2026), https://doi.org/10.1016/j.stem.2026.08.014

CellPress
OPEN ACCESS

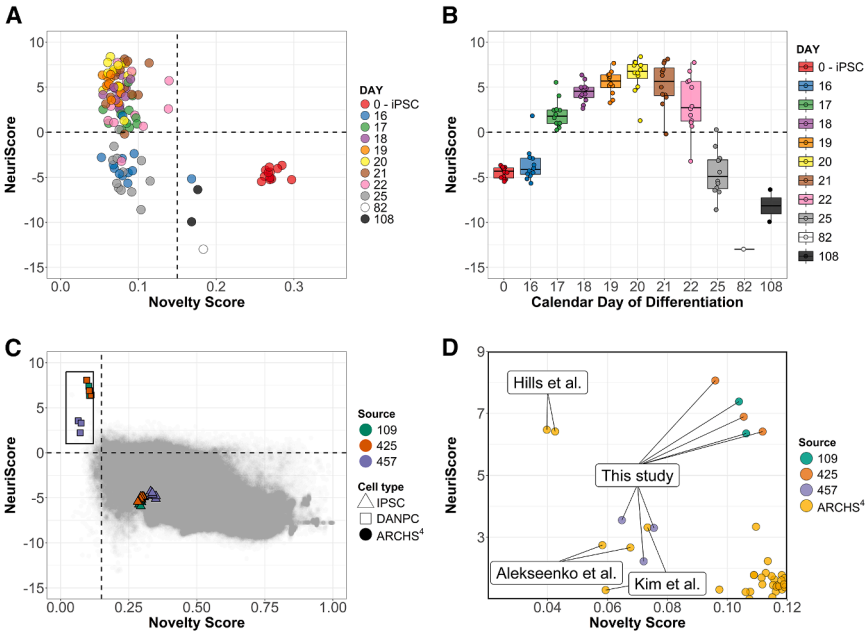

Figure 4. NeuriTest predicts DANPC identity and optimal maturity via bulk RNA-seq transcriptome features

(A) Using a timeseries differentiation, appropriate stage DANPCs were classified on the novelty score (*x* axis) and NeuriScore (*y* axis) axes with empirically derived thresholds. The NeuriScore corresponds to a maturity axis of DANPCs, while the novelty score distinguishes DANPCs from other cell types.

(B) The NeuriScore time series shows an approximately 6-day window of maturity containing cells with appropriate guilt-by-association efficacious DANPC features. Each time point is represented by up to 12 independent clones (individual dots). Data are represented as boxplots with the median as the horizontal line within each box and the interquartile range (IQR) as the lower and upper limits of the box. Whiskers extend to the most extreme observations within 1.5 × IQR.

(C) Projection of DANPC transcriptomes relative to a large background of publicly available RNA-seq samples from the ARCHS[4] compendium illustrates that validated DANPCs occupy a constrained and separable region of NeuriTest feature space (top left quadrant), distinct from a broad distribution of heterogeneous transcriptomes (bottom right quadrant).

(D) Independent published dopaminergic differentiation datasets (Hills et al.,[7] Alekseenko et al.,[22] and Kim et al.[37]) map to a similar region of NeuriTest feature space as DANPCs generated in this study, supporting biological concordance across protocols and laboratories. NeuriTest was trained exclusively on biologically validated internal datasets and was not trained using ARCHS[4] or other public data. The vertices of the inset in (C) are (x1, y1), (x2, y2) = (0.02, 1), (0.12, 9). See also Tables S1 and S6.

(deviation from typical pluripotent profiles due to genetic instability) thresholds, confirming developmental potential (Table 1; Figures 3D and S4).

Optimal neural precursor identification assay: NeuriTest

Inter-line variability in iPSC differentiation is a major hurdle in consistently identifying the optimal stage for transplantation across autologous cell products. To address this challenge, we collected gene expression profiles from cultures at multiple stages of differentiation and paired them with outcomes of animal efficacy assays to create a reference database of gene expression profiles. From these data, we developed a predictive bioinformatic assessment, "NeuriTest," to identify the optimal state of differentiation for efficacious engraftment (Figure 3D). The selection of day 18 as the representative stage for transplantation and for training the NeuriTest model was based on prior experimental evidence linking differentiation stage to *in vivo* functional efficacy.[7] In that study, iPSC-derived DANPCs from two cell lines were differentiated for either 18 or 25 days and transplanted into a rat model of PD. Although cells from both time points engrafted and generated comparable graft sizes with similar numbers of TH^+ neurons, only day 18 cells consistently reversed motor deficits. Day 25 cells failed to restore behavior, likely due to limited neurite outgrowth and poor integration into host tissue. Transcriptomic analyses demonstrated that day 18 gene expression profiles correlated with neurite extension and functional integration, supporting the designation of this stage as optimal for transplantation.

For NeuriTest, two quantitative metrics were reported: the NeuriScore and the novelty score. A sample was considered to pass if it achieved a NeuriScore ≥ 0 together with a novelty score ≤ 0.15. The NeuriScore reflects transcriptomic proximity to an empirically defined optimal differentiation window, derived from principal-component analysis of reference datasets spanning differentiation days 13, 18, and 25, with positive scores indicating similarity to the optimal, efficacious stage. The novelty score is derived from a correlation-based comparison of the global transcriptome of a test sample to an idealized DANPC reference. Lower values indicate greater transcriptomic similarity to the reference, whereas higher values indicate increasing divergence. The novelty score cutoff of 0.15 was empirically determined during NeuriTest development based on the distribution of scores observed in samples deemed appropriate or inappropriate for therapeutic use, including reference DANPC lots associated with *in vivo* efficacy and off-target or aberrantly differentiated cell populations. The 0.15 threshold is a practical identity classification boundary rather than a statistical hypothesis test; scores below this threshold indicate increasing confidence that samples are not meaningfully different from the reference DANPC phenotype at the whole-transcriptome level. Cell lots meeting both criteria were considered to have transcriptomic profiles closely matching previously validated DANPC populations and were therefore candidates suitable for further characterization studies, including efficacy and safety assessments. Figures 4A and 4B illustrates how these two metrics jointly discriminate biologically validated DANPCs from undifferentiated pluripotent cells and other nontarget cell types, while also resolving the maturation state within the DANPC lineage. To assess the ability of NeuriTest to discriminate cell types, it was used to analyze a large database of published gene expression profiles; a subset of the all RNA-seq and

Please cite this article in press as: Bratt-Leal et al., Genomic and transcriptomic quality control for an autologous iPSC-derived cell therapy for Parkinson's disease, Cell Stem Cell (2026), https://doi.org/10.1016/j.stem.2026.08.014

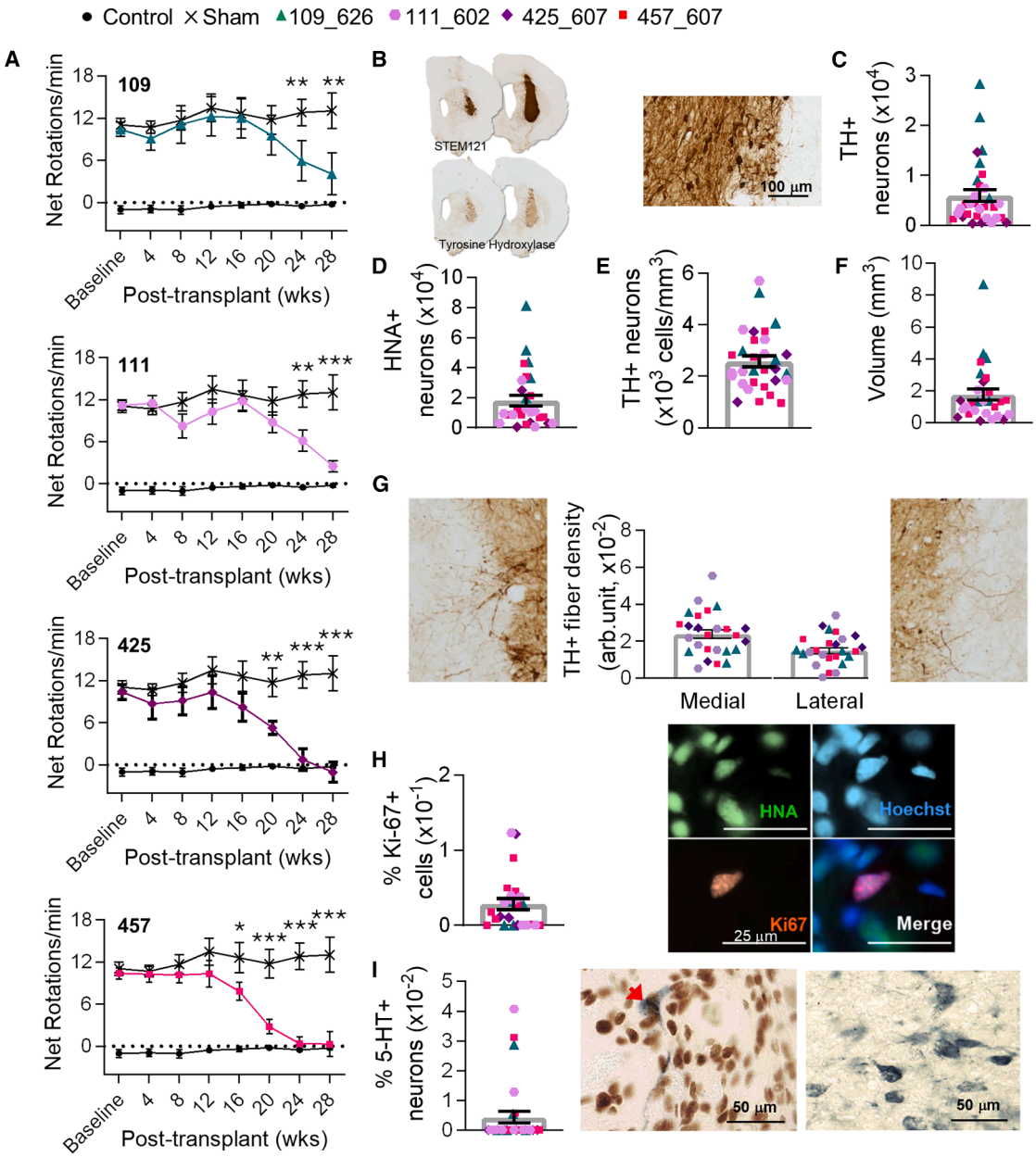

Figure 5. Engraftment and efficacy of DANPCs *in vivo* in the 6-OHDA lesioned rat hemiparkinsonian model

Rats were transplanted with DANPCs from four different iPSC lines; 109_626, 111_602, 425_607, and 457_607. The legend at the top shows symbols and colors that indicate data from each cell line; the legend applies to all behavioral analyses and all bar charts.

(A) Mean net amphetamine-induced rotations per min for rats engrafted with DANPCs derived from four different iPSC lines. From top to bottom as labeled: rats engrafted with line 109_626 cells rotated significantly less than lesioned-only rats (Sham) at 24 and 28 weeks post-graft (group × time. $F(14, 140) = 2.813$, $p = 0.001$; 24 weeks $p = 0.008$, 28 weeks $p = 0.0004$). Rats engrafted with line 111_602 cells rotated significantly less than Sham at 24 and 28 weeks post-graft (group × time. $F(14, 168) = 4.477$, $p < 0.001$; 24 weeks $p = 0.0007$, 28 weeks $p < 0.0001$). Rats engrafted with the 425_607 line cells rotated significantly less than Sham between 20 and 28 weeks post-graft (group × time. $F(14, 133) = 6.409$, $p < 0.001$; 20 weeks $p = 0.004$, 24 and 28 weeks $p < 0.0001$). Rats engrafted with line 457_607 cells rotated significantly less than Sham at 20 and 28 weeks post-graft (group × time. $F(14, 168) = 8.802$, $p < 0.001$; 16 weeks $p = 0.016$, 20–18 weeks $p < 0.0001$).

(B) Representative images of a graft immunostained for human cytoplasm marker STEM121 (top), TH (bottom), and higher magnification image of TH^+ neurons within the graft (right).

(C) Mean number of TH^+ neurons within the grafts.

(D) Mean number of HNA^+ nuclei within the grafts.

(E) Mean density of TH^+ neurons within the grafts.

(F) Mean volume of grafts (mm^3).

(legend continued on next page)

ChIP-seq sample and signature search (ARCHS^4)[36] profiles (784,581 transcriptomes) using similarly prepared RNA were used for the analysis. Figure 4C shows that the vast majority of ARCHS^4 profiles, as well as undifferentiated iPSC cultures from this study, did not pass NeuriTest. Figure 4D identifies a cluster of 14 samples that has higher NeuriScores and lower novelty scores than the other samples that are close to the cutoffs. This group consists of the 8 samples reported here as well as 2 others from our earlier work.[7] The others are published data from several reports of hPSC-derived DANPC products from other researchers, indicating that NeuriTest could have wider use as a means to qualify dopaminergic products.[22,37] The samples that were close to the NeuriTest cutoffs and displaced from the core transcriptomic profile satisfied numeric criteria but were clearly separate from the validated reference DANPCs. Most are labeled as neuronal cells from diverse experiments (Table S6) and likely reflect the inherent heterogeneity of cross-laboratory transcriptomic data, including variability in annotation conventions, mixed or transitional cell states, and partial overlap of gene expression across related lineages. These observations underscore the context dependence of threshold-based classification and highlight the importance of establishing and validating cutoffs tailored to specific differentiation protocols and reference datasets. Passing scores for both criteria were required for a sample to be considered suitable for therapeutic use. Validation with good laboratory practice (GLP)-grade cells showed a ~6-day window of optimal maturity (days 17–22), consistent with efficacy in rodent models (Figure 4; Tables 1 and S2). Further detail of the development of NeuriTest is provided as a supplemental document (Methods S1).

Efficacy study: DANPCs restored motor behavior in hemiparkinsonian rat model

DANPCs that were derived from iPSCs from four individuals with PD (109_626, 111_602, 425_607, and 457_607; Table S1) and passed all CoA-specified analytical release criteria, including NeuriTest (Table S2), were transplanted into the right striata of cyclosporine-treated Lister-hooded rats with a unilateral 6-hydroxydopamine (6-OHDA) lesion of the medial forebrain bundle.[38] A 6-OHDA lesioned control group ("Sham") received infusions consisting of vehicle only, and a surgically naive group was kept as intact controls.

There were nine decedent animals that were treated with cells during the efficacy study. All macroscopic and microscopic observations were not test material-related and were considered incidental or related to cyclosporine immunosuppression treatment. Details are provided in Figure S5A.

Amphetamine-induced rotational asymmetry was used to assess the DA imbalance between brain hemispheres pre-graft and at regular intervals post-graft until 28 weeks post-transplant.[39,40] All groups grafted with DANPCs rotated significantly less than Sham-grafted rats and, by 28 weeks post-graft, they did not differ from the intact control group (Figure 5A). These results confirm graft survival, maturation to a dopaminergic phenotype, and functional efficacy of the human cells in the grafted groups. In addition, by 28 weeks post transplantation, two animals were identified as presenting with subtle off-drug contralateral rotations and/or repetitive movements, which also serves as a surrogate marker of graft-mediated DA release.[41,42]

Immunolabeling for human-specific markers, STEM121 for human cytoplasm and anti-human nuclear antigen (HNA) for human nuclei, was used to identify transplants in all DANPC-treated groups. Typical adjacent sections of grafts labeled for STEM121 and TH are shown in Figure 5B. All grafts contained TH$^+$ dopaminergic neurons, ranging from 500, previously shown to be sufficient for functional recovery,[1] to 30,000 (Figure 5C). Recovery did not correlate to the number of TH$^+$ neurons, instead, we observed a threshold effect, as previously reported, indicating that recovery occurred in all rats harboring >500 TH$^+$ neurons.[1] Grafts contained an average of 200,000 human nuclei found at the transplant site (Figure 5D). The mean density of TH$^+$ cells in the grafts was 2,000–3,500 cells/mm^3 (Figure 5E) and grafts were ~2 mm^3 in size (Figure 5F). The ability of transplants to innervate the host brain has previously been shown to be a strong predictor of graft efficacy[7,43] and all DANPC batches produced grafts with dense dopaminergic fiber growth emanating from the graft core into host striatal tissue (Figure 5G). Human fibers labeled with STEM121 innervated brain regions distal to the graft implantation site, with some fiber projections extending approximately 5 mm posterior to the graft and innervating the host substantia nigra (Figures S5B and S5C).

Immunolabeling for proliferative human cells with Ki-67 within the transplanted brains revealed low levels for all DANPC lines (<0.15% of human cells were HNA$^+$/Ki-67$^+$, Figure 5H).

Similarly, serotonergic (5-HT) cells were found only rarely in the transplants (<0.05% of human cells were HNA$^+$/5-HT$^+$, Figure 5I).

Safety study: Transplants of DANPCs showed no tumor formation, toxicity, or abnormal biodistribution

To demonstrate the safety of our DANPC products, a 39-week tumorigenicity, toxicology, and biodistribution study was conducted with unlesioned naive animals under GLP conditions. Results are shown in Figures 6 and S6. Two DANPC lines (109_617 and 425_605) were tested at 2 doses: a low dose of 250,000 cells in 2.5 μL (LD425_605 and LD109_617) and a high dose of 500,000 cells in 5 μL (HD425_605 and HD109_617) per hemisphere. A total of 386 immunodeficient athymic nude rats

(G) Histograms of fiber density (arbitrary units) of TH$^+$ projections emanating from the medial and lateral edges of the grafts into the host brain. Representative images of TH$^+$ fibers emerging from medial (left) and lateral (right) sides of the graft.
(H) Mean percentage of Ki-67$^+$ proliferative cells within the grafts. Images of immunocytochemical staining of Ki-67$^+$ cell in graft showing nuclear localization. Ki-67 (red), HNA (green), Hoescht (blue).
(I) Images of immunocytochemical staining of 5-HT (blue) in graft (left, red arrow) and in positive control section of raphe nucleus (right). Mean percentage of 5-HT$^+$ within the grafts (bar graphs, center). Error bars = standard error of the mean. For histograms, data points represent individual grafts from each cell batch. Symbols (shown at top): black circle = naive control group; black X = Sham (rats that were lesioned but received no transplant); green triangle = cell line 109_626; lilac circle = cell line 111_602; purple diamond = cell line 425_607; pink square = cell line 457_607. *$p \leq 0.01$; **$p \leq 0.001$; ***$p \leq 0.0001$.
Scale bars: 100 μm (B), 25 μm (H), and 50 μm (I).
See also Figure S5 and Tables S1 and S2.

Please cite this article in press as: Bratt-Leal et al., Genomic and transcriptomic quality control for an autologous iPSC-derived cell therapy for Parkinson's disease, Cell Stem Cell (2026), https://doi.org/10.1016/j.stem.2026.08.014

A

Safety Study Design						
Test sample	Week 4		Week 26		Week 39	
	M	F	M	F	M	F
Vehicle control	5	5	10	10	10	10
Low dose line 109	5	5	10	10	17	17
High dose line 109	5	5	10	10	17	17
Low dose line 425	5	5	10	10	17	17
High dose line 425	5	5	10	10	17	17
10% iPSC 90% DANPC 109	-	-	-	-	10	10
10% iPSC 90% DANPC 425	-	-	-	-	10	10
100% iPSC 0% DANPC 109	-	-	-	-	10	10
100% iPSC 0% DANPC 425	-	-	-	-	10	10

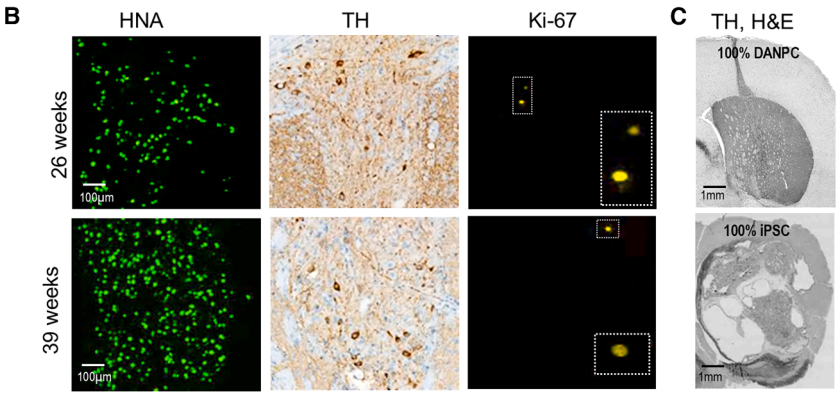

D Proliferation in grafts

Ki67/HNA (%)			
	Mean	SD	#
LD109	0.55	0.99	27
HD109	1.15	3.62	29
LD425	0.81	1.86	26
HD425	0.46	0.92	28

E Incidence of teratomas

Group	#
Vehicle control	0/20
100% DANPCs 109, 425	0/68
10% iPSC 109	0/20
10% iPSC 425	1/20
100% iPSC109	1/20
100% iPSC 425	16/20

Figure 6. Safety study

(A) Experimental design indicating the treatment groups, time points, and number of animals used for the biodistribution, toxicity, and tumorigenicity study.

(B) Representative images of sections through grafts of cell lines 109_617 and 425_605, labeled with antibodies to HNA, TH, and Ki-67. Inserts show magnification of the Ki-67-positive cells in the sections.

(C) Graft sections stained with TH and H&E showing 100% line 425_605 DANPCs (top) and teratoma from 100% undifferentiated line 109_617 iPSCs (bottom).

(D) Table indicating minimal Ki-67 proliferation for both cell lines at low and high doses.

(E) Table showing incidence of teratomas in groups with undifferentiated iPSCs spiked into the dosed DANPCs.

Scale bars: 100 µm (B) and 1 mm (C).

See also Figure S6 and Tables S1 and S2.

(7.5- to 10-week old) were randomly divided into 9 groups and an equal number of male and female rats were injected bilaterally into the striatum with vehicle (5% Flexbumin in Plasma-Lyte 148) or DANPCs formulated in vehicle. The groups were distributed as shown in Figure 6A.

In the 39-week tumorigenicity study, no test material-related deaths occurred in animals that received DANPC lines 109_617 or 425_605 at either the high or low dose. Sporadic early death/termination occurred at low incidence in the cell-treated groups and were unrelated to the treatment (Line 425_605: 4 males, 3 females; Line 109_617: 2 males, 3 females). Five rats were euthanized early due to inflammation in the prostate gland, a soft tissue sarcoma (undifferentiated sarcoma in the skin), inflammation in the lung, a keratoacanthoma, and inflammation in the vaginal submucosa. One rat was found dead and exhibited chronic progressive nephropathy upon necropsy. Another was found dead shortly after surgery and had marked inflammation at the site of injection; this death was considered a post-operative complication due to the presence of bacteria within the lesion rather than a test material effect. For five other rats, the cause of death could not be determined due to the absence of significant macroscopic or microscopic findings.

Grafts and injection sites were examined by immunohistochemistry at three time points: 4, 26, and 39 weeks. Markers examined were HNA, TH, 5-HT, and Ki-67. Human cells (HNA^+) were detected along the needle track and in the graft region at all time points and both doses of the two cell lines. Consistent with the 6-OHDA efficacy study, there was very little proliferation as detected by Ki-67 antibody (<1.15% of HNA^+ cells) (Figures 6B and 6D), while TH-positive cells were detected in the grafts at all time points (Figure 6B).

For the tumorigenicity study, DANPCs were tested for any residual undifferentiated iPSCs for their ability to form teratomas, which is the tumor type commonly derived from pluripotent stem cells.[44] Samples of 100% undifferentiated iPSCs were transplanted to rat brain to serve as a positive control, and a spike-in study was performed using 10% iPSCs mixed into the DANPCs to assess the safety margin. Transplantation of undifferentiated iPSCs from the two lines demonstrated that both

could produce teratoma tumors in the brain location shown in Figures 6C and 6E. No tumors were observed in animals that received 100% DANPCs from either of the cell lines at both high and low doses (Figure 6E). In one animal dosed with 90% 425_605 DANPCs with 10% iPSCs, there were small cellular structures that resembled a teratoma at the injection site (data not shown). No macroscopic findings were observed for 109_617 DANPCs with 10% iPSCs.

To evaluate potential toxicity of the transplanted DANPCs, animals injected with the high and low doses were assessed at all time points. There were no effects observed at any time point on body weight (Figure S6A), survival, food consumption, ophthalmology findings, clinical observations, hematology parameters, or clinical chemistry in either sex at both dose levels (data not shown). In addition, there were no reported differences in any of the neurobehavioral measures tested over the course of the study (activity, arousal, handling reactivity, posture, rearing, and vocalization) among the groups (data not shown).

The biodistribution of transplanted cells was examined by qPCR assay to detect human β-globin genomic DNA in rodent tissues. The analysis was performed on samples from the vehicle-treated group, and treated animals with high dose of line 109_617 (HD109) and high dose of line 425_605 (HD425) at weeks 26 and 39 (n = 5F + 5M per time point). There were no detectable copies of human genomic DNA found in the vehicle-treated group at either time point. For both the HD109_617- and HD425_605-treated groups at both time points, the human β-globin DNA was above the level of detection only within the brain hemispheres that were transplanted, indicating that DANPCs were confined to the brain post transplantation (Figure S6B).

DISCUSSION

Autologous iPSC-derived DANPCs offer a personalized and immunologically compatible approach for PD therapy, eliminating the need for immunosuppression required with allogeneic approaches. A key practical requirement for autologous therapies is that preclinical data establish a framework in which new donor-derived products can advance to clinical use without requiring animal studies to ensure safety and efficacy of each product. Our preclinical work with cells from six independent donors with PD, none of which were used or intended for use in patients, demonstrated consistent *in vitro* and *in vivo* performance across manufacturing lots. These studies were further supported by pilot Good Manufacturing Practices (GMP) manufacturing runs across seven iPSC lines from 3 different PD donors.

Clinical translation was enabled by demonstrating the ability to successfully generate patient-specific DANPCs that met all analytical release criteria for each donor and characterization of clonal differences or repeatability of differentiation from a particular clone was not a focus of this work. The combination of conventional flow cytometry and advanced transcriptomic analyses provides assurance that future clinical-grade lots meeting these release criteria will be safe and efficacious without additional animal testing.

In preclinical safety studies, DANPCs transplanted into immunodeficient rats remained localized to the brain without tumorigenicity or abnormal cell proliferation, unlike undifferentiated iPSC-containing samples that consistently formed teratomas, validating the sensitivity of our QC assays. DANPC grafts restored motor function to near-intact levels, with robust engraftment, maturation to dopaminergic neurons, and dense dopaminergic fiber outgrowth into host striatal tissue across multiple donor-derived batches. These data were supported by a recently published study in which we demonstrated the ability to safety and accurately target human DANPCs to the post-commissural putamen in cynomolgus macaque brain, a brain much closer in size and anatomy to humans.[45]

Two major quality control challenges for autologous iPSC therapies are genomic instability and identification of the optimal differentiation stage. We addressed the genomic instability issue by performing WGS and copy-number variant mapping at all stages of the manufacturing process, ensuring that no germline or acquired genomic mutations compromised product safety. To predict differentiation potential, we developed NeuriTest, an ML-based transcriptomic assay modeled after PluriTest. While *in vitro* assays such as NeuriTest, TH^+ cell proportion, and DA release each provide valuable information about DANPC identity and function, they capture distinct biological attributes and therefore do not necessarily rank cell preparations identically. NeuriTest is designed to assess transcriptomic identity and developmental maturity relative to DANPC populations previously shown to be efficacious *in vivo*, whereas TH expression and neurotransmitter release reflect marker expression and functional output under defined *in vitro* conditions. When viewed in the context of a broad public RNA-seq background, NeuriTest highlights similarities among validated DANPCs from published data. NeuriTest is not intended to be a stand-alone assay but is more predictive of potency than single markers and provides context for other complementary *in vitro* functional assays.

We recently reported that the efficacy of DANPCs derived from iPSCs from two different individuals and transplanted into the rat model of PD was critically dependent on the maturity of the cells. Cultures differentiated for 18 days reversed behavioral effects of dopaminergic neuron lesions in rats, but cells differentiated for 25 days did not. The day 25 cells engrafted and expressed markers of dopaminergic neurons, but they did not innervate the host and were ineffective in the rat model.[7] Because of variations in culture conditions and intrinsic genetic and epigenetic differences among iPSC clones,[46] all clones do not differentiate at the same rate, and choosing a single absolute culture time point[47] is not sufficient to meet the challenge of predicting function of each patient-derived cell line. To meet this challenge, we applied the same principles that we used in development of PluriTest to create a bioinformatic assay that would predict the likelihood of a specific culture of DANPCs to mature into functional DA neurons after transplantation.

If differences between cultures using research-grade and GMP-grade reagents are not noticed, transplanted clinical-grade cells can behave very differently than research-grade cells.[48] NeuriTest distinguishes differences in optimal transplantation time points between research-grade and GMP-grade processes (data not shown), allowing modifications to optimize transplantation. This demonstrates that an in-depth understanding of the transcriptomic trajectory throughout key differentiation time points can be used to guide development of clinical-grade cells and ensure comparability to those derived

through research-grade processes prior to initiation of costly IND-enabling animal studies. We envision further development of predictive transcriptomic assays as part of a potency assurance matrix for product release. Using the transcriptome at the transplantation stage of the product to predict downstream potential for engraftment, DA release and innervation would be invaluable for ensuring product consistency, safety, and efficacy during clinical development. The integrated use of predictive bioinformatic QC tools sets a new standard for the development and validation of autologous regenerative cell therapies, facilitating rapid and individualized cell product release for clinical applications.

The preclinical data reported here informed dose selection for the ASPIRO phase 1/2a trial (https://clinicaltrials.gov/study/NCT06344026), in which dosing of the first two cohorts of patients was completed in 2024. 12-month data from the first eight patients treated (four low dose and four high dose) in the ongoing study indicate that predefined safety and tolerability endpoints have been met, with accompanying signals consistent with preliminary clinical efficacy.[49]

The clinical goal for dopaminergic cell therapy is to replace approximately 100,000 TH^+ neurons per putamen, based on post-mortem analyses of brains from PD patients who experienced significant clinical benefit following fetal tissue transplantation.[50] In our rodent efficacy studies, the number of surviving TH^+ neurons was approximately 1%–2% of the total number of cells injected. Based on this estimate, a low dose of 5 million DANPCs per putamen would result in replacement of 50,000–100,000 TH^+ neurons, whereas a high dose of 10 million cells per putamen may yield 100,000–200,000 TH^+ neurons, thereby bracketing the therapeutic target of 100,000 TH^+ neurons depending on engraftment efficiency in humans. Together, with the 12-month data reported from the ASPIRO clinical trial, these findings support the feasibility of autologous DANPC therapy and provide a framework for advancing personalized regenerative treatments for PD and other diseases.

Limitations of the study

Like others in the field, we found that iPSC clones had variable properties. All of the samples reported here passed all quality control measures, but other samples failed early in the protocol and were terminated. The genomic quality control processes were designed to fail fast to save time and cost, but the process can be made more efficient. Simultaneous genomic analyses of multiple clones may identify additional criteria that would narrow the choices and save the costs of following several clones through all processes. NeuriTest is based on reference data derived from xenogeneic transplantation of human cells into rodent brains, which may be limited in their similarity to autologous human transplants. Because of the diversity of the human genome, we anticipate that some patient samples will not be amenable to reprogramming or differentiation. We currently use fibroblasts for reprogramming, but other sources of tissue, such as blood, may be useful to obtain quality iPSCs from every individual. Due to the limitations of current preclinical disease models and study duration, these studies cannot determine whether autologous iPSC-derived grafts may acquire disease-associated pathological features over extended periods following transplantation into patients with PD, including α-synuclein pathology or mitochondrial dysfunction. Although the genomic screening performed here excludes known pathogenic variants, it does not exclude susceptibility to sporadic disease-associated phenotypes arising from genetic, epigenetic, environmental, or age-related factors. Conversely, iPSC reprogramming has been reported to reset cellular features associated with aging[51,52] and PD pathology,[53] and the extent to which such disease-associated phenotypes may re-emerge in differentiated cells or following long-term transplantation remains to be established.

RESOURCE AVAILABILITY

Lead contact

Further information and requests for resources, data, and materials should be directed to the lead contact, Andres Bratt-Leal (abrattleal@aspenneuro.com).

Materials availability

No new reagents were generated in this study.

Data and code availability

WGS and RNA-seq and DNA SNP array data generated during this study are subject to controlled access due to donor privacy protection requirements. Data are available from the lead contact upon reasonable request, subject to a data use agreement and nondisclosure agreement. Data access is also available on approval from the European Genome and Phenome Archive (EGA: https://ega-archive.org/). The NeuriTest classifier software is available upon request, subject to a data use agreement and nondisclosure agreement. Accession numbers are listed in the key resources table. Additional data supporting the findings of this study are available in the supplemental information.

ACKNOWLEDGMENTS

We thank and acknowledge the contributions of Brendan Kelly and Rae Pass for surgery support and data collection for the rodent efficacy study, Gerry Deckert for help with handling genomic data, Alyssa Holman for RNA-seq data analysis, and Bernhard Schuldt and Franz-Josef Muller for advice in the construction of the early versions of NeuriTest. We also thank Meghan Bliss-Moreau for developing early versions of flow cytometry assays; Jason Stein and Aditi Shankar for *in vitro* culture support and Patricia Lopes, Mei Bueno, Dana Arthur for their support of the pilot manufacturing runs; Jeanne Bonelle for her support envisioning and starting a quality program; and Stan Roberts for consulting support with the GLP safety study. We acknowledge and thank Charles River Labs for their execution of the GLP rodent study. We thank David Barker for advice and support. Research was supported by Aspen Neuroscience and the California Institute for Regenerative Medicine (DISC2P-11595). We are grateful to the Summit for Stem Cell Foundation for monetary support in the early phases of this work. The graphical abstract was created using BioRender.

AUTHOR CONTRIBUTIONS

The authors confirm contribution to the paper as follows: conception and design, A.M.B.-L., T.G., R.M.W., M.J.L., J.F.L., and E.D.W.; performance of experiments, data collection, and analysis, J.A.M., R.H., H.T., D.B., D.F., A.Z., C.P., C.L., D.T., C.B., D.R.W., and B.C.; interpretation of results, A.M.B.-L., T.G., R.M.W., J.A.M., R.H., D.B., G.B., D.F., A.Z., Y.L., C.C., D.R.W., U.N., E.L.L., M.J.L., E.D.W., and X.Z.; managed the projects, A.M.B.-L., T.G., D.R.W., R.M.W., M.J.L., and X.Z.; draft manuscript preparation A.M.B.-L., T.G., R.M.W., J.A.M., R.H., G.B., D.F., C.L., Y.L., C.C., D.T., M.J.L., J.F.L., and X.Z.; and all authors reviewed the results, gave input to the manuscript, and approved the final version of the manuscript.

DECLARATION OF INTERESTS

J.F.L. is co-founder, shareholder and scientific advisor for Aspen Neuroscience, Inc. and a stockholder and scientific advisor for Savannah BioTherapeutics,

Conception Bio, Stembiosys, Kadimastem, Retro Biosciences, and Mangrove Neuro, as well as receives royalty payments for a license of patent US 8,442,772 to Thermo Fisher, Inc. A.M.B.-L., T.G., R.M.W., J.A.M., H.T., D.B., G.B., D.F., C.P., C.L., Y.L., C.C., D.T., U.N., E.D.W., and X.Z. are employees and shareholders of Aspen Neuroscience, Inc. A.Z., D.R.W., and B.C. are shareholders and former employees of Aspen Neuroscience, Inc. Aspen Neuroscience, Inc. is the sponsor of the ASPIRO clinical trial. C.B., E.L.L., and M.J.L. were supported by funding from Aspen Neuroscience, Inc.

A.M.B.-L., H.T., J.F.L., J.A.M., and R.M.W. are named as inventors on a patent application owned by Aspen Neuroscience entitled "Methods of differentiating neural cells and related compositions and methods of use" (US 2023/0059010). A.M.B.-L., J.F.L., and R.M.W. are named inventors on a patent application owned by Aspen Neuroscience entitled "Methods of identifying dopaminergic neurons and progenitor cells" (US 2022/0254448). J.F.L. is a named inventor on a patent assigned to Aspen Neuroscience entitled "Compositions and methods for defining cells" (US 8,442,772). D.B., J.A.M., and R.M.W. are named inventors on a patent application owned by Aspen Neuroscience entitled "Methods of classifying the differentiation state of cells" (US 2023/0377685). C.L. and D.F. are named as inventors on a patent application owned by Aspen Neuroscience entitled "Potency assay matrix for neuronal cells" (US application no. 19/206,993).

STAR★METHODS

Detailed methods are provided in the online version of this paper and include the following:

- KEY RESOURCES TABLE
- EXPERIMENTAL MODEL AND STUDY PARTICIPANT DETAILS
  - Human subjects
  - Animals and housing conditions, efficacy study
  - Animals and housing conditions, GLP safety study
- METHOD DETAILS
  - Fibroblast derivation, culture, iPSC generation and maintenance
  - Differentiation of iPSCs to DANPCs
  - Whole-genome sequencing
  - Genetic identity matching
  - Genomic integrity and Copy Number Variant (CNV) screening
  - Somatic mutation analysis in iPSCs and DANPCs
  - Neuronal differentiation and validation using NeuriTest
  - Flow cytometry
  - Sterility and endotoxin testing
  - Post-thaw cell concentration and viability
  - Quantitative Real-Time Polymerase Chain Reaction (qRT-PCR)
  - *In vitro* detection of iPSCs spiked into DANPCs
  - Immunocytochemistry
  - Neurotransmitter release quantification
  - Surgical procedures, efficacy study
  - Behavioral assessments, efficacy study
  - Immunohistochemistry, efficacy study
  - Surgical procedures, GLP safety study
  - Biodistribution testing, GLP safety study
  - Necropsy, histopathology and immunohistochemistry, GLP safety study
- QUANTIFICATION AND STATISTICAL ANALYSIS
  - Statistical Analysis

SUPPLEMENTAL INFORMATION

Supplemental information can be found online at https://doi.org/10.1016/j.stem.2026.08.014.

Received: October 29, 2025
Revised: May 20, 2026
Accepted: August 26, 2026

REFERENCES

1. Grealish, S., Diguet, E., Kirkeby, A., Mattsson, B., Heuer, A., Bramoulle, Y., Van Camp, N., Perrier, A.L., Hantraye, P., Björklund, A., et al. (2014). Human ESC-derived dopamine neurons show similar preclinical efficacy and potency to fetal neurons when grafted in a rat model of Parkinson's disease. Cell Stem Cell *15*, 653–665. https://doi.org/10.1016/j.stem.2014.09.017.
2. Barker, R.A., Björklund, A., and Parmar, M. (2024). The history and status of dopamine cell therapies for Parkinson's disease. BioEssays *46*, e2400118. https://doi.org/10.1002/bies.202400118.
3. Barker, R.A., Lao-Kaim, N.P., Guzman, N.V., Athauda, D., Bjartmarz, H., Björklund, A., Church, A., Cutting, E., Daft, D., Dayal, V., et al. (2025). The TransEuro open-label trial of human fetal ventral mesencephalic transplantation in patients with moderate Parkinson's disease. Nat. Biotechnol. *44*, 70–78. https://doi.org/10.1038/s41587-025-02567-2.
4. Kefalopoulou, Z., Politis, M., Piccini, P., Mencacci, N., Bhatia, K., Jahanshahi, M., Widner, H., Rehncrona, S., Brundin, P., Björklund, A., et al. (2014). Long-term clinical outcome of fetal cell transplantation for Parkinson disease: two case reports. JAMA Neurol. *71*, 83–87. https://doi.org/10.1001/jamaneurol.2013.4749.
5. Clark, B.J., Lelos, M.J., and Loring, J.F. (2024). Advancing Parkinson's disease treatment: cell replacement therapy with neurons derived from pluripotent stem cells. Stem Cells *42*, 781–790. https://doi.org/10.1093/stmcls/sxae042.
6. Doi, D., Magotani, H., Kikuchi, T., Ikeda, M., Hiramatsu, S., Yoshida, K., Amano, N., Nomura, M., Umekage, M., Morizane, A., et al. (2020). Pre-clinical study of induced pluripotent stem cell-derived dopaminergic progenitor cells for Parkinson's disease. Nat. Commun. *11*, 3369. https://doi.org/10.1038/s41467-020-17165-w.
7. Hills, R., Mossman, J.A., Bratt-Leal, A.M., Tran, H., Williams, R.M., Stouffer, D.G., Sokolova, I.V., Sanna, P.P., Loring, J.F., and Lelos, M.J. (2023). Neurite Outgrowth and Gene Expression Profile Correlate with Efficacy of Human Induced Pluripotent Stem Cell-Derived Dopamine Neuron Grafts. Stem Cells Dev. *32*, 387–397. https://doi.org/10.1089/scd.2023.0043.
8. Jeon, J., Cha, Y., Hong, Y.J., Lee, I.H., Jang, H., Ko, S., Naumenko, S., Kim, M., Ryu, H.L., Shrestha, Z., et al. (2025). Pre-clinical safety and efficacy of human induced pluripotent stem cell-derived products for autologous cell therapy in Parkinson's disease. Cell Stem Cell *32*, 343–360.e7. https://doi.org/10.1016/j.stem.2025.01.006.
9. Park, S., Park, C.W., Eom, J.H., Jo, M.Y., Hur, H.J., Choi, S.K., Lee, J.S., Nam, S.T., Jo, K.S., Oh, Y.W., et al. (2024). Preclinical and dose-ranging assessment of hESC-derived dopaminergic progenitors for a clinical trial on Parkinson's disease. Cell Stem Cell *31*, 25–38.e8. https://doi.org/10.1016/j.stem.2023.11.009.
10. Song, B., Cha, Y., Ko, S., Jeon, J., Lee, N., Seo, H., Park, K.J., Lee, I.H., Lopes, C., Feitosa, M., et al. (2020). Human autologous iPSC-derived dopaminergic progenitors restore motor function in Parkinson's disease models. J. Clin. Invest. *130*, 904–920. https://doi.org/10.1172/JCI130767.
11. Piao, J., Zabierowski, S., Dubose, B.N., Hill, E.J., Navare, M., Claros, N., Rosen, S., Ramnarine, K., Horn, C., Fredrickson, C., et al. (2021). Preclinical Efficacy and Safety of a Human Embryonic Stem Cell-Derived Midbrain Dopamine Progenitor Product, MSK-DA01. Cell Stem Cell *28*, 217–229.e7. https://doi.org/10.1016/j.stem.2021.01.004.
12. Kirkeby, A., Nelander, J., Hoban, D.B., Rogelius, N., Bjartmarz, H., , et al.; Novo Nordisk Cell Therapy R&D, Storm, P., Fiorenzano, A., Adler, A.F., Vale, S. (2023). Preclinical quality, safety, and efficacy of a human embryonic stem cell-derived product for the treatment of Parkinson's disease, STEM-PD. Cell Stem Cell *30*. 1299–1314 e1299. https://doi.org/10.1016/j.stem.2023.08.014.
13. Sawamoto, N., Doi, D., Nakanishi, E., Sawamura, M., Kikuchi, T., Yamakado, H., Taruno, Y., Shima, A., Fushimi, Y., Okada, T., et al. (2025). Phase I/II trial of iPS-cell-derived dopaminergic cells for

Parkinson's disease. Nature *641*, 971–977. https://doi.org/10.1038/s41586-025-08700-0.

14. Tabar, V., Sarva, H., Lozano, A.M., Fasano, A., Kalia, S.K., Yu, K.K.H., Brennan, C., Ma, Y., Peng, S., Eidelberg, D., et al. (2025). Phase I trial of hES cell-derived dopaminergic neurons for Parkinson's disease. Nature *641*, 978–983. https://doi.org/10.1038/s41586-025-08845-y.
15. Chang, J.W., Na, H.K., Chang, K.W., Park, C.W., Kim, D.H., Park, S., Park, C.Y., Eom, J.H., Nam, S.T., Jo, K.S., et al. (2025). Phase 1/2a clinical trial of hESC-derived dopamine progenitors in Parkinson's disease. Cell *188*, 7036–7048.e11. https://doi.org/10.1016/j.cell.2025.09.010.
16. Lee, A.Y., Jeong, J., Heo, K.-N., Park, S., Ah, Y.-M., Han, J.M., Lee, J.-Y., and Min, S.I. (2025). Complications Associated with Immunosuppressive Agents in Solid Organ Transplant Recipients: A Nationwide Analysis. J. Clin. Med. *14*, 3602. https://doi.org/10.3390/jcm14103602.
17. Tao, Y., Vermilyea, S.C., Zammit, M., Lu, J., Olsen, M., Metzger, J.M., Yao, L., Chen, Y., Phillips, S., Holden, J.E., et al. (2021). Autologous transplant therapy alleviates motor and depressive behaviors in parkinsonian monkeys. Nat. Med. *27*, 632–639. https://doi.org/10.1038/s41591-021-01257-1.
18. Wang, S., Zou, C., Fu, L., Wang, B., An, J., Song, G., Wu, J., Tang, X., Li, M., Zhang, J., et al. (2015). Autologous iPSC-derived dopamine neuron transplantation in a nonhuman primate Parkinson's disease model. Cell Discov. *1*, 15012. https://doi.org/10.1038/celldisc.2015.12.
19. Hallett, P.J., Deleidi, M., Astradsson, A., Smith, G.A., Cooper, O., Osborn, T.M., Sundberg, M., Moore, M.A., Perez-Torres, E., Brownell, A.L., et al. (2015). Successful function of autologous iPSC-derived dopamine neurons following transplantation in a non-human primate model of Parkinson's disease. Cell Stem Cell *16*, 269–274. https://doi.org/10.1016/j.stem.2015.01.018.
20. Schweitzer, J.S., Song, B., Herrington, T.M., Park, T.Y., Lee, N., Ko, S., Jeon, J., Cha, Y., Kim, K., Li, Q., et al. (2020). Personalized iPSC-Derived Dopamine Progenitor Cells for Parkinson's Disease. N. Engl. J. Med. *382*, 1926–1932. https://doi.org/10.1056/NEJMoa1915872.
21. Müller, F.J., Schuldt, B.M., Williams, R., Mason, D., Altun, G., Papapetrou, E.P., Danner, S., Goldmann, J.E., Herbst, A., Schmidt, N.O., et al. (2011). A bioinformatic assay for pluripotency in human cells. Nat. Methods *8*, 315–317. https://doi.org/10.1038/nmeth.1580.
22. Alekseenko, Z., Dias, J.M., Adler, A.F., Kozhevnikova, M., van Lunteren, J.A., Nolbrant, S., Jeggari, A., Vasylovska, S., Yoshitake, T., Kehr, J., et al. (2022). Robust derivation of transplantable dopamine neurons from human pluripotent stem cells by timed retinoic acid delivery. Nat. Commun. *13*, 3046. https://doi.org/10.1038/s41467-022-30777-8.
23. Fedele, S., Collo, G., Behr, K., Bischofberger, J., Müller, S., Kunath, T., Christensen, K., Gündner, A.L., Graf, M., Jagasia, R., et al. (2017). Expansion of human midbrain floor plate progenitors from induced pluripotent stem cells increases dopaminergic neuron differentiation potential. Sci. Rep. *7*, 6036. https://doi.org/10.1038/s41598-017-05633-1.
24. Chambers, S.M., Fasano, C.A., Papapetrou, E.P., Tomishima, M., Sadelain, M., and Studer, L. (2009). Highly efficient neural conversion of human ES and iPS cells by dual inhibition of SMAD signaling. Nat. Biotechnol. *27*, 275–280. https://doi.org/10.1038/nbt.1529.
25. Beqqali, A., Kloots, J., Ward-van Oostwaard, D., Mummery, C., and Passier, R. (2006). Genome-wide transcriptional profiling of human embryonic stem cells differentiating to cardiomyocytes. Stem Cells *24*, 1956–1967. https://doi.org/10.1634/stemcells.2006-0054.
26. Tano, K., Yasuda, S., Kuroda, T., Saito, H., Umezawa, A., and Sato, Y. (2014). A novel in vitro method for detecting undifferentiated human pluripotent stem cells as impurities in cell therapy products using a highly efficient culture system. PLoS One *9*, e110496. https://doi.org/10.1371/journal.pone.0110496.
27. Laurent, L.C., Ulitsky, I., Slavin, I., Tran, H., Schork, A., Morey, R., Lynch, C., Harness, J.V., Lee, S., Barrero, M.J., et al. (2011). Dynamic changes in the copy number of pluripotency and cell proliferation genes in human ESCs and iPSCs during reprogramming and time in culture. Cell Stem Cell *8*, 106–118. https://doi.org/10.1016/j.stem.2010.12.003.
28. Andrews, P.W., Barbaric, I., Benvenisty, N., Draper, J.S., Ludwig, T., Merkle, F.T., Sato, Y., Spits, C., Stacey, G.N., Wang, H., et al. (2022). The consequences of recurrent genetic and epigenetic variants in human pluripotent stem cells. Cell Stem Cell *29*, 1624–1636. https://doi.org/10.1016/j.stem.2022.11.006.
29. Avery, S., Hirst, A.J., Baker, D., Lim, C.Y., Alagaratnam, S., Skotheim, R.I., Lothe, R.A., Pera, M.F., Colman, A., Robson, P., et al. (2013). BCL-XL mediates the strong selective advantage of a 20q11.21 amplification commonly found in human embryonic stem cell cultures. Stem Cell Rep. *1*, 379–386. https://doi.org/10.1016/j.stemcr.2013.10.005.
30. Garitaonandia, I., Amir, H., Boscolo, F.S., Wambua, G.K., Schultheisz, H.L., Sabatini, K., Morey, R., Waltz, S., Wang, Y.C., Tran, H., et al. (2015). Increased risk of genetic and epigenetic instability in human embryonic stem cells associated with specific culture conditions. PLoS One *10*, e0118307. https://doi.org/10.1371/journal.pone.0118307.
31. Merkle, F.T., Ghosh, S., Kamitaki, N., Mitchell, J., Avior, Y., Mello, C., Kashin, S., Mekhoubad, S., Ilic, D., Charlton, M., et al. (2017). Human pluripotent stem cells recurrently acquire and expand dominant negative P53 mutations. Nature *545*, 229–233. https://doi.org/10.1038/nature22312.
32. Mandelker, D., and Ceyhan-Birsoy, O. (2020). Evolving Significance of Tumor-Normal Sequencing in Cancer Care. Trends Cancer *6*, 31–39. https://doi.org/10.1016/j.trecan.2019.11.006.
33. Vales, J.P., and Barbaric, I. (2024). Culture-acquired genetic variation in human pluripotent stem cells: Twenty years on. BioEssays *46*, e2400062. https://doi.org/10.1002/bies.202400062.
34. Panopoulos, A.D., D'Antonio, M., Benaglio, P., Williams, R., Hashem, S.I., Schuldt, B.M., DeBoever, C., Arias, A.D., Garcia, M., Nelson, B.C., et al. (2017). iPSCORE: A Resource of 222 iPSC Lines Enabling Functional Characterization of Genetic Variation across a Variety of Cell Types. Stem Cell Rep. *8*, 1086–1100. https://doi.org/10.1016/j.stemcr.2017.03.012.
35. International Stem Cell Initiative (2018). Assessment of established techniques to determine developmental and malignant potential of human pluripotent stem cells. Nat. Commun. *9*, 1925. https://doi.org/10.1038/s41467-018-04011-3.
36. Lachmann, A., Torre, D., Keenan, A.B., Jagodnik, K.M., Lee, H.J., Wang, L., Silverstein, M.C., and Ma'ayan, A. (2018). Massive mining of publicly available RNA-seq data from human and mouse. Nat. Commun. *9*, 1366. https://doi.org/10.1038/s41467-018-03751-6.
37. Kim, T.W., Piao, J., Koo, S.Y., Kriks, S., Chung, S.Y., Betel, D., Socci, N.D., Choi, S.J., Zabierowski, S., Dubose, B.N., et al. (2021). Biphasic Activation of WNT Signaling Facilitates the Derivation of Midbrain Dopamine Neurons from hESCs for Translational Use. Cell Stem Cell *28*, 343–355.e5. https://doi.org/10.1016/j.stem.2021.01.005.
38. Guimarães, R.P., Ribeiro, D.L., Dos Santos, K.B., Godoy, L.D., Corrêa, M.R., and Padovan-Neto, F.E. (2021). The 6-hydroxydopamine Rat Model of Parkinson's Disease. J. Vis. Exp. e62923. https://doi.org/10.3791/62923.
39. Björklund, A., and Dunnett, S.B. (2019). The Amphetamine Induced Rotation Test: A Re-Assessment of Its Use as a Tool to Monitor Motor Impairment and Functional Recovery in Rodent Models of Parkinson's Disease. J. Parkinsons Dis. *9*, 17–29. https://doi.org/10.3233/JPD-181525.
40. Dunnett, S.B., and Torres, E.M. (2012). Rotation in the 6-OHDA-Lesioned Rat. In Animal Models of Movement Disorders, *61*, E.L. Lane and S.B. Dunnett, eds. (Humana Press), pp. 299–315. https://doi.org/10.1007/978-1-61779-298-4_15.
41. Breger, L.S., Dunnett, S.B., and Lane, E.L. (2013). Comparison of rating scales used to evaluate l-DOPA-induced dyskinesia in the 6-OHDA lesioned rat. Neurobiol. Dis. *50*, 142–150. https://doi.org/10.1016/j.nbd.2012.10.013.
42. Lloyd, K., Lawton, M., and Whone, A. (2023). Practically Defined Off-State Dyskinesia Following Repeated Intraputamenal Glial Cell Line-Derived Neurotrophic Factor Administration. Mov. Disord. *38*, 104–112. https://doi.org/10.1002/mds.29262.

43. Steinbeck, J.A., Choi, S.J., Mrejeru, A., Ganat, Y., Deisseroth, K., Sulzer, D., Mosharov, E.V., and Studer, L. (2015). Optogenetics enables functional analysis of human embryonic stem cell-derived grafts in a Parkinson's disease model. Nat. Biotechnol. *33*, 204–209. https://doi.org/10.1038/nbt.3124.

44. Peterson, S.E., Tran, H.T., Garitaonandia, I., Han, S., Nickey, K.S., Leonardo, T., Laurent, L.C., and Loring, J.F. (2011). Teratoma generation in the testis capsule. J. Vis. Exp. e3177. https://doi.org/10.3791/3177.

45. Emborg, M.E., Mancinelli, A., Colwell, J.C., Zinnen, A.D., Pape, B., Brunner, K., Bondarenko, V., Fitz, C., Coonen, J., Menna, V., et al. (2024). Preclinical evaluation of transaxial intraputaminal trajectory for enhanced distribution of grafted cells in Parkinson's disease. J. Neurosurg. *141*, 1554–1566. https://doi.org/10.3171/2024.4.JNS24367.

46. Cooke, J.A., Voigt, A.P., Collingwood, M.A., Stone, N.E., Whitmore, S.S., DeLuca, A.P., Burnight, E.R., Anfinson, K.R., Vakulskas, C.A., Reutzel, A.J., et al. (2023). Propensity of Patient-Derived iPSCs for Retinal Differentiation: Implications for Autologous Cell Replacement. Stem Cells Transl. Med. *12*, 365–378. https://doi.org/10.1093/stcltm/szad028.

47. Hiller, B.M., Marmion, D.J., Thompson, C.A., Elliott, N.A., Federoff, H., Brundin, P., Mattis, V.B., McMahon, C.W., and Kordower, J.H. (2022). Optimizing maturity and dose of iPSC-derived dopamine progenitor cell therapy for Parkinson's disease. NPJ Regen. Med. *7*, 24. https://doi.org/10.1038/s41536-022-00221-y.

48. Temple, S., and Studer, L. (2017). Lessons Learned from Pioneering Neural Stem Cell Studies. Stem Cell Rep. *8*, 191–193. https://doi.org/10.1016/j.stemcr.2017.01.024.

49. Aspen Neuroscience. (2026). Aspen Neuroscience Announces Positive 12-Month Data from its ASPIRO Clinical Trial in a Late-Breaking Oral Presentation at the AD/PD 2026 International Conference on Alzheimer's and Parkinson's Diseases. https://aspenneuroscience.com/aspen-neuroscience-announces-positive-12-month-data-from-its-aspiro-clinical-trial-in-a-late-breaking-oral-presentation-at-t/.

50. Hagell, P., and Brundin, P. (2001). Cell survival and clinical outcome following intrastriatal transplantation in Parkinson disease. J. Neuropathol. Exp. Neurol. *60*, 741–752. https://doi.org/10.1093/jnen/60.8.741.

51. Lapasset, L., Milhavet, O., Prieur, A., Besnard, E., Babled, A., Aït-Hamou, N., Leschik, J., Pellestor, F., Ramirez, J.M., De Vos, J., et al. (2011). Rejuvenating senescent and centenarian human cells by reprogramming through the pluripotent state. Genes Dev. *25*, 2248–2253. https://doi.org/10.1101/gad.173922.111.

52. Prigione, A., Hossini, A.M., Lichtner, B., Serin, A., Fauler, B., Megges, M., Lurz, R., Lehrach, H., Makrantonaki, E., Zouboulis, C.C., et al. (2011). Mitochondrial-associated cell death mechanisms are reset to an embryonic-like state in aged donor-derived iPS cells harboring chromosomal aberrations. PLoS One *6*, e27352. https://doi.org/10.1371/journal.pone.0027352.

53. Drouin-Ouellet, J., Legault, E.M., Nilsson, F., Pircs, K., Bouquety, J., Petit, F., Shrigley, S., Birtele, M., Pereira, M., Storm, P., et al. (2022). Age-related pathological impairments in directly reprogrammed dopaminergic neurons derived from patients with idiopathic Parkinson's disease. Stem Cell Rep. *17*, 2203–2219. https://doi.org/10.1016/j.stemcr.2022.08.010.

54. Danecek, P., Bonfield, J.K., Liddle, J., Marshall, J., Ohan, V., Pollard, M.O., Whitwham, A., Keane, T., McCarthy, S.A., Davies, R.M., and Li, H. (2021). Twelve years of SAMtools and BCFtools. Gigascience *10*, giab008. https://doi.org/10.1093/gigascience/giab008.

55. Stringer C., Wang T., Michaelos M. Pachitariu M. Cellpose: a generalist algorithm for cellular segmentation. *Nat Methods.* 2021;18:100–106. doi:10.1038/s41592-020-01018-x.

56. Stirling, D.R., Swain-Bowden, M.J., Lucas, A.M., Carpenter, A.E., Cimini, B.A., and Goodman, A. (2021). CellProfiler 4: improvements in speed, utility and usability. BMC Bioinformatics *22*, 433. https://doi.org/10.1186/s12859-021-04344-9.

57. Patro, R., Duggal, G., Love, M.I., Irizarry, R.A., and Kingsford, C. (2017). Salmon provides fast and bias-aware quantification of transcript expression. Nat. Methods *14*, 417–419. https://doi.org/10.1038/nmeth.4197.

58. Dobin, A., Davis, C.A., Schlesinger, F., Drenkow, J., Zaleski, C., Jha, S., Batut, P., Chaisson, M., and Gingeras, T.R. (2013). STAR: ultrafast universal RNA-seq aligner. Bioinformatics *29*, 15–21. https://doi.org/10.1093/bioinformatics/bts635.

59. Pakstis, A.J., Gandotra, N., Speed, W.C., Murtha, M., Scharfe, C., and Kidd, K.K. (2021). The population genetics characteristics of a 90 locus panel of microhaplotypes. Hum. Genet. *140*, 1753–1773. https://doi.org/10.1007/s00439-021-02382-0.

60. Rajeevan, H., Soundararajan, U., Kidd, J.R., Pakstis, A.J., and Kidd, K.K. (2011). ALFRED: an allele frequency resource for research and teaching. Nucleic Acids Res. *40*, D1010–D1015. https://doi.org/10.1093/nar/gkr924.

61. Benvenisty, N., Draper, J.S., Gokhale, P.J., Healy, L., Hewitt, Z., Hursh, D., Hodgson, A., Ludwig, T.E., Mah, N., McClelland, S.E., et al. (2025). A call to action for deciphering genetic variants in human pluripotent stem cells for cell therapy. Cell Stem Cell *32*, 508–512. https://doi.org/10.1016/j.stem.2025.03.003.

62. Bolon, B., Garman, R.H., Pardo, I.D., Jensen, K., Sills, R.C., Roulois, A., Radovsky, A., Bradley, A., Andrews-Jones, L., Butt, M., et al. (2013). STP position paper: Recommended practices for sampling and processing the nervous system (brain, spinal cord, nerve, and eye) during nonclinical general toxicity studies. Toxicol. Pathol. *41*, 1028–1048. https://doi.org/10.1177/0192623312474865.

Please cite this article in press as: Bratt-Leal et al., Genomic and transcriptomic quality control for an autologous iPSC-derived cell therapy for Parkinson's disease, Cell Stem Cell (2026), https://doi.org/10.1016/j.stem.2026.08.014

STAR★METHODS

KEY RESOURCES TABLE

REAGENT or RESOURCE	SOURCE	IDENTIFIER
Antibodies		
Alexa Fluor® 647 mouse anti-human TRA-1-81 antibody	BD Biosciences	560793; RRID: AB_10550550
Anti-5HT (serotonin) antibody	Immunostar	20080; RRID: AB_572263
Anti-HNF-3b Antibody	Santa Cruz Biotechnology	SC-374376; RRID: AB_10989742
Anti-Human Nuclei antibody (235-1)	Millipore	MAB1281; RRID: AB_94090
Anti-Ki-67 antibody	Abcam	Ab15580; RRID: AB_443209
Anti-STEM 121 antibody	Takara	Y40410; RRID: AB_2801314
Anti-Tyrosine Hydroxylase Antibody	Millipore	AB152; RRID: AB_390204
BV421 mouse anti-OCT-3/4 antibody	BD Bioscience	565644; RRID: AB_2739320
Discovery CC1	Ventana	950-500
Discovery Hematoxylin	Ventana	760-2021
Donkey anti-Mouse IgG (H+L) Highly Cross-Adsorbed Secondary Antibody, Alexa Fluor™ 555	Invitrogen	A31570; RRID:AB_2536180
Donkey Anti-Rabbit IgG (H+L) Highly Cross-Adsorbed Secondary Antibody, Alexa Fluor™ 488	Invitrogen	A21206; RRID:AB_2535792
Goat anti-Mouse IgG (H+L) Highly Cross-Adsorbed Secondary Antibody, Alexa Fluor 488	Invitrogen	A11029; RRID: AB_2534088
Goat anti-Rabbit IgG (H+L) Highly Cross-Adsorbed Secondary Antibody, Alexa Fluor 594	Invitrogen	A11037; RRID: AB_2534095
Goat Anti-Rabbit IgG Antibody (H+L), Biotinylated	Vector Laboratories	BA-1000; RRID: AB_2313606
Hoechst 33342, trihydrochloride trihydrate	Invitrogen	H3570; RRID:AB_3675235
Horse Anti-Mouse IgG Antibody, rat adsorbed (H+L), Biotinylated	Vector Laboratories	BA-2001, RRID: AB_2336180
Monoclonal Mouse Anti-Human Nucleoli antibody [NM95]	Abcam	Ab-190710; RRID: AB_2937055
Monoclonal Rabbit Anti-Ki-67 antibody [SP6]	Abcam	Ab-16667; RRID: AB_302459
Omnimap anti-Ms HRP	Ventana	760-4310; RRID:AB_2885182
Omnimap Anti-Rb HRP	Ventana	760-4311; RRID:AB_2811043
PE anti-human FOXA2 antibody	Miltenyi	130-123-779; RRID: AB_2921755
FITC anti-human OTX2 antibody	Miltenyi	130-121-186; RRID: AB_2801805
PerCP-Cy5.5 mouse anti-human PAX6 antibody	BD Biosciences	562388; RRID: AB_11153319
Polyclonal Rabbit anti-Tyrosine Hydroxylase antibody	Pel-Freez Biologicals	P40101; RRID: AB_2313713
Chemicals, peptides, and recombinant proteins		
(+)-Methamphetamine hydrochloride	Sigma-Aldrich	M8750
1X DPBS, no calcium, no magnesium	Gibco	14190144
2-mercaptoethanol	Gibco	21985023; CAS:60-24-2
3,3′-Diaminobenzidine	Sigma-Aldrich	D8001
6-Hydroxydopamine hydrobromide	Sigma-Aldrich	H116
B-27 Supplement (50X), serum free	Gibco	17504044

(*Continued on next page*)

Please cite this article in press as: Bratt-Leal et al., Genomic and transcriptomic quality control for an autologous iPSC-derived cell therapy for Parkinson's disease, Cell Stem Cell (2026), https://doi.org/10.1016/j.stem.2026.08.014

CellPress
OPEN ACCESS

Continued

REAGENT or RESOURCE	SOURCE	IDENTIFIER
BDNF	BioTechne	248-GMP-025; CAS: 218441-99-7
Bovine Fibronectin	Sigma-Aldrich	F1141
Bovine Serum Albumin	Fisher	BP1600-100; CAS: 9048-46-8
cGMP HSA 25% Solution	Akron Bio	AK8228-0100
CHIR99021	BioTechne	TB4423-GMP; CAS: 252917-06-9
Collagenase B	Roche	11088807001; CAS: 9001-12-1
CryoStor CS10	Stemcell Technologies	07930
DAPT	BioTechne	TB2634-RMU/10; CAS: 208255-80-5
dibutyl-cAMP	Sigma-Aldrich	28745; CAS: 16980-89-5
DMEM, High Glucose + GlutaMAX	Gibco	10566016
DMEM/F-12, HEPES	Gibco	11330057
Donkey Serum	Sigma-Aldrich	D9663
DPX Mountant	Sigma-Aldrich	06522
Essential™ 8 Medium	Gibco	A15169
Fetal Bovine Serum (FBS), ES Cell-Qualified	Gibco	16141-079
Flexbumin	Takeda	2G0201
GDNF	BioTechne	212-GMP-050
GlutaMAX Supplement	Gibco	35050061
HBSS, no calcium, no magnesium, no phenol red	Gibco	14175095
Human Fibronectin solution (plasma-derived, viral inactivated, GMP)	Akron Biotech	AK9930-0001
Hydrogen Peroxide 30%	Sigma-Aldrich	1072090250
Insulin	Sigma-Aldrich	I9278; CAS: 11061-68-0
KnockOut Serum Replacement	Gibco	10828028
L-Ascorbic acid	Sigma-Aldrich	A4544; CAS: 50-81-7
L-Glutamine (200 mM)	Gibco	25030081
LDN 193189	BioTechne	TB6053/10; CAS: 1435934-00-1
MEM Non-Essential Amino Acids Solution (100X)	Gibco	11140050
Methanol	Sigma-Aldrich	A452-1; CAS: 64-56-1
Methanol, Extra Pure, SLR	Fisher Scientfic	10214490
Mouse Laminin	Sigma-Aldrich	L2020; CAS: 114956-81-9
mTESR1	Stem Cell Technologies	85850
N-2 Supplement (100X)	Gibco	17502048
Neurobasal Medium, Minus Phenol Red	Gibco	12348017
Normal Goat Serum	Thermo Fisher Scientific	31873; RRID: AB_2532167
Normal Horse Serum	Thermo Fisher Scientific	31874; RRID: AB_2532168
PlasmaLyte A 148 solution	Baxter	JB2544
Poly-L-ornithine hydrobromide	Sigma-Aldrich	P3655; CAS: 27378-49-0
Potassium chloride	Sigma-Aldrich	P9541; CAS: 7447-40-7
Primocin	Invivogen	ANT-PM-1
Prolong Diamond Antifade Mountant with DAPI	Invitrogen	P36962
Prolong Gold Antifade Mountant	Invitrogen	P36930
Purmorphamine	Sigma Aldrich	540220; CAS: 483367-10-8
Reagent A100 Lysis Buffer	Chemometec	910-0003
Reagent B Stabilizing Buffer	Chemometec	910-0002
Recombinant Laminin-511 E8 fragment (iMatrix-511MG)	Matrixome	892005

(*Continued on next page*)

Continued

REAGENT or RESOURCE	SOURCE	IDENTIFIER
SB 431542	BioTechne	TB1614-GMP; CAS: 301836-41-9
Sodium Chloride 0.9% IV solution 500ml	Baxter	FKE1323
Sonic hedgehog C25II	BioTechne	464-SH-200/CF
StemPro Accutase Cell Dissociation Reagent	Gibco	A11105-01
TGFβ3	BioTechne	243-GMP-025
Triton X-100	Sigma-Aldrich	X100
Trizma Base	Sigma-Aldrich	T1503
UltraPure™ 0.5M EDTA, pH 8.0	Invitrogen	15575020
Xylene	Fisher Scientific	10385910
Y27632 dihydrochloride	BioTechne	TB1254-GMP; CAS: 129830-38-2
Critical commercial assays		
Chromomap DAB	Ventana	760-159
CTS CytotuneTM-iPSC 2.1 Sendai Reprogamming kit	ThermoFisher Scientific	A34546
Discovery FAM kit	Ventana	760-243
Discovery Rhodamine kit	Ventana	760-233
eBioscience FoxP3/transcription factor staining buffer set	ThermoFisher Scientific	00-5523-00
High-Capacity cDNA Reverse Transcription kit	Applied Biosystems	4374966
Infinium Global Screening Array v2.0	Illumina	20005132
miRNeasy Mini kit	Qiagen	217004
MycoSeq PCR Detection kit	Applied Biosystems	4460626
Sendai quantification kit	ThermoFisher Scientific	A50190
Taqman Gene Expression Master Mix	Applied Biosystems	4369016
VECTASTAIN Elite ABC-HRP kit	Vector Laboratories	PK-6100; RRID: AB_2336819
Vector® SG Substrate kit, Peroxidase (HRP)	Vector Laboratories	SK-4700
Zombie Aqua™ fixable viability kit	Biolegend	423101
Deposited data		
RNA-seq	European genome-phenome archive (EGA)	ARCHIVE deposit # EGA:EGAD50000002281, EGA:EGAD50000002282, EGA:EGAD50000002283
Whole genome sequencing	European genome-phenome archive (EGA)	ARCHIVE deposit # EGA:EGAD50000002280
Experimental models: Cell Lines		
293T	ATCC	CRL-3216
Experimental models: Organisms/strains		
Crl:NIH-Fox1rnu	Charles River Laboratory	316
Lister Hooded Rat	Charles River Laboratory	Crl:LIS RRID: RGD_2312466
Oligonucleotides		
ACTB VIC-MGB_PL	ThermoFisher Scientific	Hs01060665_g1
H-glo-F4 Forward Primer: 5'-GTCATAGGAAGGGGATAAGTAACAG-3'	This paper	N/A
H-glo-P4 Probe: 5'-TCATTCGTCTGTTTCCCATTCT-3'	This paper	N/A
H-glo-R4 Reverse Primer: 5'-TGAGACTTCCACACTGATGCA-3'	This paper	N/A
Primer: POU5F1 Forward: GATGGCGTACTGTGGGCCC	Piao, Jinghua et al.[11]	N/A
Primer: POU5F1 Reverse: TGGGACTCCTCCGGGTTTTG	Piao, Jinghua et al. [11]	N/A

(*Continued on next page*)

Continued

REAGENT or RESOURCE	SOURCE	IDENTIFIER
Probe: POU5F1: CCAAGGCGGCTTGGAGACCT-FAM-MGB	Piao, Jinghua et al. [11]	N/A
VRTN FAM-MGB	ThermoFisher Scientific	Hs00217248_m1
Software and algorithms		
ALFRED database	Yale University	https://alfred.med.yale.edu/
bcftools Github v1.9	Danecek et al.[54]	https://github.com/samtools/bcftools
Cellpose	Stringer et al.[55]	https://www.cellpose.org/
CellProfiler	Stirling et al.[56]	https://cellprofiler.org/
ClinVar database NCBI version 2021 v.	NCBI	https://www.ncbi.nlm.nih.gov/clinvar/
FlowJo	BD Life Sciences	https://www.flowjo.com/
GraphPad Prism	GraphPad Software	https://www.graphpad.com/
NeuriTest™ classifier	This paper	available upon request
PhenoLOGIC	Revvity	https://www.revvity.com/
QuantStudio™ Real -Time PCR Software v1.4	ThermoFisher Scientific	N/A
Salmon v1.1.0	Patro et al.[57]	https://github.com/COMBINE-lab/salmon
STAR aligner v2.7.3a	Dobin et al.[58]	https://github.com/alexdobin/STAR
Visiopharm 2019.05 or 2020: Image Analysis Software	Visiopharm	https://visiopharm.com
Zen lite	Zeiss	https://www.zeiss.com/
Other		
Bx50 microscope	Olympus Optical Co.	BX50-FL-PA
ND8000 Spectrophotometer v2.0	ThermoFisher Scientific	ND-800-GL
QIAsymphony SP	Qiagen	9001297
QuantStudio™ 7 Flex Real-Time PCR System	Applied Biosystems	N/A
S60 digital slide scanner	Hamamatsu	N/A
Zeiss Axioscan slide scanner	Zeiss	N/A

EXPERIMENTAL MODEL AND STUDY PARTICIPANT DETAILS

Human subjects

Donation of cellular material: Subjects diagnosed with Parkinson's disease were enrolled under IRB-approved protocol HSC-08-5109 (Scripps Research) and provided written informed consent for research and commercial uses of their samples. The IRB approval was renewed each year. Exclusion criteria included the presence of known pathogenic PD-associated mutations as identified by genomic screening (Table S3). The donor numbers and genders are listed in Table S1. Donor age and demographic information are not disclosed to protect donor privacy.

Animals and housing conditions, efficacy study

Female lister-hooded rats (Crl:LIS) between 8-10 weeks old were purchased from Charles River and housed with ad libitum access to food/water on a 14-hour (light)/10-hour (dark) photoperiod. Testing was conducted during the light cycle period only. Primary enclosures were as specified in the RSPCA and LASA, 2015, Guiding Principles on Good Practice for Animal Welfare and Ethical Review Bodies (M. Jennings Ed.). All experiments were conducted in accordance with the requirements of the UK Animal Scientific Procedures Act, 1986, under Home Office PPL P49E8C976 and under local ethics board approval. All surgical procedures were carried out under induction of surgical plane anesthesia by delivery of 2.5-5% isoflurane in 1L/min O_2. Veterinary approved analgesics were administered, and appropriate post-operative care and checks were performed.

Animals and housing conditions, GLP safety study

The GLP toxicity, tumorigenicity and biodistribution study was performed at Charles River Laboratories. A total of 386 naïve athymic nude rats (Crl:NIH-Fox1rnu strain from Charles River Laboratories, Wilmington, North Carolina) was used with a 1:1 ratio of males and females. The animals were paired or individually housed in solid bottomed cages with a ventilated micro-isolator filtering system at 68-79°F with a humidity of 30-70% with a 12-hour (light)/12-hour (dark) photoperiod and unrestricted access to sterilized water and irradiated block PicoLab® Diet food pellets. Each animal was identified using a subcutaneously implanted electronic identification chip. The animals were approximately 7.5 to 10 weeks old and weighed between 114 and 303 grams at initiation of dosing. Males and

females were randomized separately and assigned to groups upon receipt. All study animals were subject to weekly assessments of body weight and food consumption and detailed clinical observations throughout the duration of the study.

METHOD DETAILS

Fibroblast derivation, culture, iPSC generation and maintenance

The fibroblasts were isolated from a skin punch biopsy collected from donors under an IRB-approved protocol as described previously.[7] The frozen fibroblast cells were thawed and seeded into a fibronectin-coated plate with fibroblast medium. For reprogramming, the fibroblast cells were transduced using Sendai virus containing the Yamanaka factors (CTS™ Cytotune™-iPSC 2.1 Sendai Reprogramming kit, ThermoFisher Scientific).

Differentiation of iPSCs to DANPCs

A vial of iPSCs was thawed, cultured on Laminin-511-E8 (Matrixome) coated plates and passaged when reaching the confluency of 60% or greater. Cells may be passaged up to 8 times in mTeSR1 (StemCell Technologies) in preparation for the differentiation and were seeded at 305,000 cells/cm^2 with rho kinase inhibitor Y-27632 at a concentration of 10 μM (BioTechne). From day 0 through day 10, cells were cultured in a basal differentiation medium consisting of a 1:1 mix of DMEM/F-12 (Gibco) and Neurobasal (Gibco) medium supplemented with 0.5x N2 (Gibco), 0.5x B27 (Gibco), 1x NEAA (Gibco), 1x GlutaMax (Gibco), insulin (Sigma-Aldrich, 2.5μg/mL), β-mercaptoethanol (Gibco, 50μM), and L-glutamine (Gibco, 1mM). On days 0-1, LDN 193189 (BioTechne, 100nM), SB431542 (BioTechne, 10mM), and KOSR (Thermo Fisher, 5%) were added to basal neural induction medium and replaced daily. Beginning on day 1, SHH (BioTechne, 100ng/mL) and Purmorphamine (Sigma-Aldrich, 2μM) were added and maintained through day 6. KOS was reduced to 2% on day 2 and continued through day 10, LDN was maintained from day 0 through day 10, and SB was used only through day 4. CHIR99021 (BioTechne, 2 μM) was introduced on day 2 and maintained through day 10. Starting on day 11, the basal medium was changed to 1X Neurobasal supplemented with 1X B27, 1X N2, 1X NEAA, and 1X GlutaMax. From days 11–20, BDNF (BioTechne, 20ng/mL), ascorbic acid (Sigma-Aldrich, 0.2mM), GDNF (BioTechne, 20ng/mL), dbcAMP (Sigma-Aldrich, 0.5mM), TGFβ3 (BioTechne, 1ng/mL), and DAPT (BioTechne, 10μM) were added to the basal medium and medium was changed daily, with the exception of day 18. CHIR (2μM) was continued for days 11–12 and then discontinued. ROCK inhibitor Y-27632 (10 μM) was added on day 16 when cells were passaged using Accutase (Innovative Cell Technologies) and replated at a 1:2 ratio onto Laminin-511-E8 coated plates. On day 20, the cells were harvested with Accutase, washed and pooled as DANPCs, formulated in CryoStor CS10 (BioLife Solutions), and cryopreserved with a Via Freeze controlled-rate freezer (Cytiva).

Whole-genome sequencing

For PD mutation screening genomic DNA was extracted from subject derived fibroblasts by using the Qiagen DNeasy Blood & Tissue kits, according to the manufacturer's instructions. Genomic DNA (gDNA) libraries were prepared by using the ABclonal Rapid Plus DNA Lib Prep kit. gDNA was sequenced following the manufacturers protocol to produce paired end 2x150 bp reads targeting an average depth of 30X coverage using Illumina NovaseqX. Whole-genome sequencing was performed at an average depth of ~30× coverage. While FDA draft guidance for human allogeneic cell-based products recommends ≥50× coverage, this recommendation is intended for highly expanded allogeneic cell banks, where extensive proliferation increases the risk of acquiring low-frequency somatic variants. In contrast, the autologous iPSC-derived products described here are manufactured with limited expansion and are clonally derived, substantially reducing the likelihood of subclonal variant accumulation. In addition, the genomic quality control framework implemented in this study is designed as a fail-fast system incorporating orthogonal screening layers, including SNP-based identity confirmation, copy-number variant prescreening, and transcriptome-based functional qualification. Sequencing at ~30× coverage was therefore considered sufficient and appropriate for detection of clinically relevant single-nucleotide, structural, and copy-number variants within this manufacturing context, consistent with prior regulatory interactions. Reads were aligned to the GRCh38 (hg38) reference genome using the DRAGEN system (Illumina) with default parameters (see command below). Germline variants were called and annotated with ClinVar (https://www.ncbi.nlm.nih.gov/clinvar/). Subjects with pathogenic variants associated with PD were excluded (Table S3).

The following command was used to process and call variants in the WGS data:

```
/opt/edico/bin/dragen
-f
-r /staging/human/reference/hg38/dragen_hg38_cnv_rna/
-1 /staging/work/fastq/"$sample$suffix1''
-2 /staging/work/fastq/"$sample$suffix2''
–RGID Illumina_RGID
–RGSM "$sample"
–output-directory "$sample_dir"
–output-file-prefix "$sample"
–enable-duplicate-marking true
–enable-variant-caller true
–enable-map-align-output true
```

–enable-cnv true
–cnv-enable-self-normalization true
–intermediate-results-dir /staging/intermediate/
–enable-sv true
–enable-metrics-compression true
–cnv-enable-plots true
–qc-cross-cont-vcf /opt/edico/config/sample_cross_contamination_resource_hg38.vcf.gz
–qc-coverage-region-1 /regions_repeats_removed_plus_1_right_padding.bed
–qc-coverage-reports-1 cov_report full_res

Genetic identity matching

DNA was obtained from oral swabs at the time of skin biopsy, fibroblast cultures, iPSC clones, and DANPCs. This was followed by genotyping using Global Screening Array v2 (Illumina, San Diego, US) as per the manufacturer's protocol. Eighty-one SNPs with high heterozygosity, low linkage disequilibrium, and a low fixation index[59] were used for subject identity confirmation. SNP B-allele frequencies (BAF) were regressed between oral DNA and derivative samples. A match was defined as $R^2 \geq 0.98$. SNP characteristics were confirmed with ALFRED (https://alfred.med.yale.edu/ALFRED/index.jsp;[60]).

Genomic integrity and Copy Number Variant (CNV) screening

CNV analysis was performed on GSA genotyping array data. CNV calling used bcftools cnv with default parameters. An in-house reference array was used to normalize calls. CNV burdens exceeding 30Mbp on any autosome were flagged as QC failures.

Somatic mutation analysis in iPSCs and DANPCs

Variant annotations used for genomic quality control were derived from curated public databases, including ClinVar and cancer driver gene resources, and were reviewed at defined clinical and manufacturing milestones. As variant interpretation evolved over time, updated releases of these databases were periodically reviewed, and newly classified pathogenic or likely pathogenic variants were evaluated for their potential impact on product safety prior to release of clinical lots. This framework enables incorporation of newly identified risk variants into the genomic quality control workflow as part of clinical progression, rather than relying on static variant lists.

Interpretation of genomic variants is inherently constrained by the current state of knowledge and available reference databases. Many detected variants are classified as variants of unknown significance (VUS), for which pathogenicity may not yet be established and may evolve over time as additional functional and clinical data become available. As highlighted recently,[61] conclusions regarding genomic safety must be understood in the context of continuously evolving variant annotation frameworks. In this study, genomic assessments were designed to identify variants with established clinical relevance; however, it remains possible that variants currently classified as benign or of unknown significance may be reclassified in the future. To mitigate this limitation, our quality control strategy incorporates periodic re-evaluation of variant interpretation at defined clinical progression milestones, allowing newly identified or reclassified pathogenic variants to be incorporated into ongoing safety assessments of clinical lots.

De novo somatic mutation screening was performed on WGS data from iPSCs and DANPCs. Oncogenic variants including 22 genes and 2,417 candidate variants were curated from the Genomic Data Commons Data Portal Brain Cancer dataset (https://portal.gdc.cancer.gov/) deduplicated to 2,329 unique positions (Table S4). Neurology-relevant variants consisted of genes curated by Gene Ontology terms "brain development" (GO:0007420) and "cellular response to dopamine" (GO:1903351), totaling 862 unique genes; 410 genes had ClinVar pathogenic entries spanning 20,841 unique positions after deduplication. Overlaps with any known pathogenic mutation were manually reviewed (Table S3).

Neuronal differentiation and validation using NeuriTest

Total RNA was isolated from DANPC cultures with RNAeasy. cDNA library construction was conducted using the NEBNext UltraTM II RNA Library Prep kit (Illumina) with poly A enrichment. The prepared libraries were sequenced on an Novaseq6000 (Illumina) with paired end 2x150 bp reads (up to 30 million reads).

Document S1 provides a more detailed description of the NeuriTest tool. Reads were aligned to the gencode.v32.transcripts.fa reference transcriptome with the Salmon pseudoaligner v1.1.0.[57] NeuriTest analysis was performed to assess DANPC consistency and maturity, implemented in R v4.3.3. Reference training data was derived from multiple DA differentiation time courses and rodent efficacy studies. Three analytical steps were performed: Gene set identification of maturity-specific and universal baseline gene sets; Novelty Score quantifying global similarity to reference DANPCs (pass $\leq$0.15); NeuriScore ranking maturity against the optimal timing for transplantable DANPCs (pass $\geq$0). Classification required passing both thresholds. Varying DANPC samples with the same maturity consistently passed, while other less mature samples generally failed due to off-target maturity. The application of NeuriScore and Novelty Score metrics to classify transcriptomic identity and maturation state across differentiation stages and cell types is illustrated in Figure 4.

Flow cytometry

iPSC and DANPC identity were measured by multi-color flow cytometry. $2x10^6$ of either iPSC or DANPC cells in suspension were treated with the live/dead Zombie Aqua^{TM} fixable viability kit (Biolegend, 423101), then iPSC cell suspensions were stained with Alexa

Fluor® 647 mouse anti-human TRA-1-81 antibody (BD Biosciences, 560793) followed by fixation and permeabilization using eBioscience FoxP3/transcription factor staining buffer set (ThermoFisher Scientific, 00-5523-00) iPSC cells were then stained with BV421 mouse anti-OCT–3/4 antibody (BD Bioscience, 565644). DANPC cell suspensions were fixed and permeabilized using eBioscience FoxP3/transcription factor staining buffer set (ThermoFisher Scientific, 00-5523-00), then stained with PE anti-human FOXA2 antibody (Miltenyi, 130-123-779), FITC anti-human OTX2 antibody (Miltenyi, 130-121-186) and PerCP-Cy5.5 mouse anti-human PAX6 antibody (BD Biosciences, 562388). Cells were analyzed with a FACSCanto II (BD Bioscience) flow cytometer and data was analyzed with FlowJo software (BD Bioscience). Each time the flow cytometry assay for DANPC identity is performed, 293T control cells with known PAX6 expression are assayed to ensure accurate measurement of PAX6, along with staining control samples that exclude the FOXA2 antibody for accurate gating analysis.

Sterility and endotoxin testing

Sterility testing was performed at a contracted testing laboratory (Charles River Laboratories) using the United States Pharmacopeia (USP) <71> compliant 14-day culture method. Mycoplasma testing was performed at a contracted testing laboratory (Bionique Testing Laboratories Inc.) using Applied Biosystems MycoSeq PCR Detection kit, preceded by a 6-day broth enrichment to increase assay sensitivity. The Limulus Amebocyte Lysate (LAL) method was used to detect and/or qualify bacterial endotoxin in samples. 25 μL/well of samples were added into all four wells of endotoxin cartridge (Charles River Laboratories, PTS20005F), Endosafe® Nexgen-PTSTM Kinetic Reader (Charles River Laboratories) was used to measure the endotoxin level according to manufacturer's protocol.

Post-thaw cell concentration and viability

Frozen cells were thawed using ThawSTAR® Automated Cell Thawing System (Astero Bio.), 100 μL of cell suspension was mixed with 100 μL of reagent A100 lysis buffer (Chemometec) and 100 μL of reagent B stabilizing buffer (Chemometec), the prepared samples were loaded in Vial-1 cassette™ (Chemometec) and measured by NucleoCounter® NC-200 cell counter according to the manufacturer's protocol (Chemometec).

Quantitative Real-Time Polymerase Chain Reaction (qRT-PCR)

Total RNA was extracted from iPSC or DANPC using miRNease Mini kit (Qiagen) and 1 μg of RNA was converted to cDNA using high-capacity cDNA reverse transcription kit with RNase inhibitor (Applied Biosystems). To quantify the residual Sendai virus in iPSC, Taqman qRT-PCR was performed on the iPSC cDNA using custom Sendai quantification kit (ThermoFisher Scientific). To quantify residual undifferentiated iPSC levels, reference samples were prepared by diluting total RNA isolated from iPSCs at 1%, 0.1% and 0.01% into negative control RNA from fibroblasts. 1 μg of reference sample RNA and DANPC RNA were converted into cDNA, and qRT-PCR was performed by using two primer/probe sets: *POU5F1* and *VRTN* (ThermoFisher Scientific, 4331182_HS00217248_m1) with beta-Actin (*ActB*) (ThermoFisher Scientific, 4448491_HS01060665_g1) as the housekeeping reference gene. The delta Ct (dCt) was calculated by taking the difference between the Ct of the target gene and the house-keeping gene in each sample. By comparing the dCt value of the test sample with the reference sample, a higher dCt of the test sample indicates that there were fewer than 0.1% iPSCs present.

In vitro detection of iPSCs spiked into DANPCs

DANPCs spiked with increasing concentrations of iPSCs were cultured at 37°C in iPSC growth culture conditions to confirm qRT-PCR detection of residual iPSCs. 6-well plates were coated with iMatrix-511e8 (Matrixome) and maintained with mTeSR1 (Gibco) for four days in culture plates followed by subsequent visual inspection for formation of iPSC colonies.

Immunocytochemistry

DANPCs were thawed and plated in maturation medium supplemented with Y-27632 (BioTechne). Cells were passaged on days 25 and 30 and plated into a 24-well plate with glass coverslips at 200,000 cells/cm^2 in maturation medium supplemented with Y-27632. Cells were fixed in 4% Paraformaldehyde (PFA) at room temperature (RT) for 15 minutes, then washed 3 times with 1X DPBS before being blocked with a solution of 0.1% Triton-X 100, 1% BSA (Fisher), and 2.5% donkey serum (Sigma-Aldrich) in 1X DPBS for 30 minutes. Cells were incubated with primary antibodies for TH (1:500, Millipore, AB152) and FOXA2 (1:150, SCBT, SC-374376) diluted in blocking solution at 4°C overnight, then washed 3 times in 1X DPBS before being stained with secondaries the following day. Cells were incubated in fluorophore conjugated secondary antibodies (1:1000, Invitrogen, A21206 and 1:500, Invitrogen, A31570) diluted in blocking solution for 2 hours at RT, then washed 2 times with 1X DPBS. Nuclei were labeled with Hoechst (Invitrogen, H3570) at 1:10,000 in PBS for 5 minutes at RT. Cells were washed 1 more time before removing the coverslips from the well and mounting onto microscope slides (Fisher, 1255015) with ProLong Gold antifade reagent (Invitrogen, P36930).

Slides were imaged at 10x magnification on an Olympus VS200 Slide Scanner microscope with 3 representative fields of view per coverslip. Nuclear antigen FOXA2 and Hoechst were quantified with CellProfiler using the IdentifyPrimaryObjects module. Cellpose, a generalist algorithm for cellular segmentation, was trained on >3000 cells for quantifying TH-positive soma. Quantification is shown as the percentage of TH+Hoechst+ or FOXA2+Hoechst+ over the total number of Hoechst positive cells.

Neurotransmitter release quantification

To evaluate the dopaminergic and serotonergic neurons characteristics in DANPCs, a Xevo TQ-S UPLC-MS/MS assay was qualified by Pharmaron Inc. to quantify dopamine (DA) and serotonin (5-HT) in supernatant matrices. Samples were collected from DANPCs

cultured for 60 days and assayed to quantify the neurotransmitters DA and 5-HT secreted into the medium upon stimulation with KCl in a buffered salt solution (Hanks' balanced salt solution, HBSS). First, the cell culture medium was discarded, the cells were washed with HBSS, then fresh HBSS was added, and a sample was collected 30 minutes later as a baseline. Then, fresh HBSS with 56 mM KCl was added to stimulate the cells, and a sample was collected 30 minutes later. Cells were stored at 37°C during culture and stimulation.

Surgical procedures, efficacy study

To mimic late-stage PD, dopaminergic cells of the nigro-striatal pathway were unilaterally depleted by 1 μl/min infusion of 18.75 μg 6-hydroxydopamine (6-OHDA; Sigma-Aldirch 162957) with 0.025% ascorbic acid stabilizer, into the median forebrain bundle (MFB) at stereotaxic coordinates: AP= 4 mm, ML= -1.3 mm (taken from bregma) and DV= -7 mm (from dura), TB set to -3.2. Toxin was allowed to diffuse for 2 minutes before withdrawal of cannula.

On the day of transplantation, cells were thawed and formulated into a cell suspension of 150,000 cells/μl in Plasmalyte A (Baxter, JB2544) with 5% human serum albumin (Akron Bio., AK8228- 0100) as vehicle. A trypan blue viability assay was conducted on all cell suspensions prior to transplantation with a release criterion of >70% viability. Cell suspensions were kept on ice until time of use and injected unilaterally at 2 depths into the lesioned striatum at coordinates: AP= +0.6, ML= -3 and DV = -4 (depth 1) and -5 (depth 2). 1.5μL cell suspension was infused at 1μl/min at each depth, to ensure 450,000 cells/transplant, and the suspension was allowed to diffuse for 2 minutes before withdrawal of delivery cannula. Rejection of grafts was prevented by intraperitoneal (IP) injection of immunosuppressant cyclosporine A (Sandimmune, Novartis) at 10mg/kg every 24 hours, beginning 2 days prior to cell transplantation.

Behavioral assessments, efficacy study

Amphetamine-induced rotation bias testing was used post-lesion to confirm success of the unilateral MFB lesion. Rotation bias testing was conducted with 2.5 mg/kg dopamine agonist methamphetamine (Sigma-Aldrich) and undertaken every four weeks for the duration of the 28-week post-graft period. An automated rotometer set up was used to assess rotational asymmetry in an unbiased manner. Animals were required to meet ≥6 amphetamine-induced rotations per minute for inclusion in the study at baseline and were group matched according to this score. Off-drug behavior was also video recorded every 4 weeks for the duration of the 28-week post-graft period. Abnormal involuntary movements (AIMs) were scored from 10-minute videos taken at 12-, 20-, 24- and 28-weeks post grafting by an experienced researcher, blinded to group allocation. AIMs scoring consisted of assigning a score of 1-3 to reflect the amplitude or intensity of the following behaviors: axial twisting, forelimb or hindlimb dyskinesia, orolingual dyskinesia and contralateral locomotion. Behaviors were assessed in 3, 1-minute slots, over a 10-minute period off drug.

Immunohistochemistry, efficacy study

Animals were sacrificed at 28 weeks post transplantation by IP injection of pentobarbital and transcardially perfused with PBS before perfusion with 250 ml 4% PFA. Brains were post-fixed for 4 hours in 4% PFA before cryopreservation in 25% sucrose. 30 μm sections were collected on a freezing sledge microtome in a 1/12 series. For immunolabelling, a 1/12 or 1/6 series of floating sections was blocked for peroxidase reactivity (by 5 minutes incubation with 3% methanol and 3% H2O2), and non-specific binding action (by inclusion of 1-3% goat serum in blocking and antibody solutions). Permeabilization of tissue was achieved by addition of 0.1% Triton X-100 (Sigma-Aldrich) into blocking and primary solutions.

The primary antibodies for staining were human nuclei (1:2,000, Millipore MAB1281), human cytoplasm (STEM121, 1:3000, Takara Y40410), tyrosine hydroxylase (1:1,000, Millipore YAB152), Ki-67 (1:1,000 Abcam AB15580), and serotonin (5-HT, 1:10,000, Immunostar 20080). For fluorometric stains, secondary antibodies were tagged with either green (488nm, 1:200, Invitrogen A11037) or red (594 nm, 1:200, Invitrogen A11029) fluorescent probes. For colorimetric stains, biotinylated secondary antibodies for mouse (1:200, Vector Labs, BA-2001) or rabbit (1:200, Vector Labs BA-1000) were used and the signal was amplified by application of avidin-biotin (Vector labs, PK6100) before treatment with DAB (Sigma-Aldrich, D8001-5G). For double labelling, an alternative blue stain (Vector SG) was used according to manufacturer's protocol (SK-4700). All fluorometric labels were co-labelled with Hoechst 33342 (Thermofisher, 62249) to label cell nuclei. Sections were mounted on gelatin-coated slides and dried at ambient temperature overnight, before being cover-slipped with DPX (Sigma-Aldrich). Whole slides stained with STEM121, TH, and HNA/5-HT double stain were scanned at 2.5x using a Zeiss Axioscan slide scanner. Zenlite software was used to generate volume measurements using STEM121-stained sections. Two-dimensional quantification was carried out using an automated stage and stereology module NEWCAST™ from Visiopharm Integrator System software (Visiopharm, UK) on an Olympus Bx50 microscope (Olympus Optical Co., Ltd, Japan). A stereological estimate of the total numbers of human cells was generated using a 1/12 series of HNA-positive cells using an optical fractionator to sample 5% of the region of interest (the grafted area). The stereological formula $C = \Sigma c \times (\Sigma A / \Sigma a) \times f$, where Σc= the total numbers of cells counted for each animal, ΣA = the sum of all the inclusion areas for each animal, Σa= the sum of all the sample areas for each animal (number of samples areas x size of sampling frame), and f= frequency of tissue, i.e. 12 for a 1/12 series. The total numbers of TH-positive and 5-HT-positive cells were estimated by counting all labelled cells within either a 1/6 or 1/12 series and multiplying by 6 or 12, respectively. Optical density (OD) measures were obtained from 2.5x slide scanned images using Zenlite software and converting the OI measure into OD using the formulae OD=log10(IO/IT), where IO=optical intensity and IT=transmitted intensity. Using slides stained with STEM121, a 100 μm^2 bounding box was placed over the following regions of interest frontal cortex (fCTX), Nucleus Accumbens

(NAc), Globus Pallidus (GP), Amygdala (Amyg), Subthalamic nucleus/Median forebrain bundle (STN/MFB), Cerebral Peduncle (CP) and Substantia Nigra (SN). This OD was subtracted from a control region with only background staining, white matter tracts in the brain hemisphere contralateral to the transplant, to give the relative increase in OD for STEM121 fibers. Using TH immunolabelled slides, the OD of TH+ graft projections into the host striatum was evaluated at 500 μm, both medially and laterally from the transplant border.

Analysis of projections into the host striatum was conducted 500 μm from graft edge in both a medial and lateral direction using TH immunolabelled sections. A 1/12 series, double-stained for fluor-Ki-67/HNA was imaged at 20x magnification using an Opera Phenix system with Harmony imaging software (both from PerkinElmer). High throughput image analysis using the PhenoLOGIC machine learning algorithm was used to quantify the percentage of graft-derived proliferative cells (Ki-67-positive/HNA-positive) after 28 weeks maturation.

Surgical procedures, GLP safety study

Cells were thawed and formulated into a cell suspension of 100,000 cells/μl in Plasma-Lyte 148 (Baxter, JB2544) with 5% Flexbumin (Takeda, 2G0201) that was used as the vehicle control group. Cell suspensions were kept at 4°C until time of use and administered via bilateral intrastriatal injection at coordinates relative to bregma: Rostral = +0.6 mm, Lateral=3.0 mm and Dorso-Ventral= -5.0 mm (site 1) and -4.0 mm (site 2) once on Day 0. Infusion of 1.25 or 2.5 μL injection was at the rate of 0.5 μL/min on each site in both hemispheres. The needle was left in place for approximately 2 minutes before retracting.

Biodistribution testing, GLP safety study

For the high dose (HD) 425, 109, and vehicle groups, tissues, bone marrow and blood were analyzed for biodistribution of human cells using qPCR at 26- and 39-weeks post-dosing. Validated bioanalysis assay was developed to detect the target human β-globin sequence. Blood samples were collected in tubes containing K_2EDTA from at least 5 animals/sex/group via cardiac puncture at each scheduled necropsy for qPCR analysis. DNA was extracted from the samples and a qPCR assay was performed to detect human cells using the forward, reverse and probe primer sequences: 5'-GTCATAGGAAGGGGATAAGTAACAG-3' and 5'-TGAGACT TCCACACTGATGCA-3' and 5'-TCATTCGTCTGTTTCCCATTCT-3'. Duplicate QC samples were prepared at 10^4 (QC-High), 10^3 (QC-Mid), and 10^2 (QC-Low) copies of iPSC pellet DNA in a background of 1,000 ng rat liver DNA per reaction. When possible, the tissue and bone marrow DNA samples were tested at 1,000 ng per reaction while the plasma DNA samples were tested at 5 μL per reaction.

Necropsy, histopathology and immunohistochemistry, GLP safety study

Animals were euthanized by carbon dioxide inhalation. Following euthanasia, animals were perfused with 0.9% saline. Representative samples of the tissues (left brain, heart, left kidney, liver, lung, lymph node [left cervical, left mandibular, and mesenteric], spleen, ovaries or testes, and cervical spinal cord) were collected from all animals and preserved in 10% neutral buffered formalin. The eyes (including the optic nerve) were preserved in Davidson's fixative (Sigma-Aldrich, H0290). The testes and epididymides were preserved in Davidson's fixative. Tissues were embedded in paraffin, sectioned, mounted on glass slides, and stained with hematoxylin and eosin. Animals were subjected to a complete necropsy examination, which included evaluation of the carcass and musculoskeletal system, all external surfaces and orifices, cranial cavity and external surfaces of the brain, and thoracic, abdominal, and pelvic cavities with their associated organs and tissues. The animals were examined for external abnormalities including palpable masses. Four 1 mm brain sections, two rostral and two caudal to the rostral cut of the standard CRL brain section 2 (sampling and preparation according to Bolon et al.[62] Both hemispheres of the brain were trimmed for all non-perfused duration of study (DOS) animals; the left hemisphere was trimmed for the perfused euthanized *in extremis* and scheduled animals. The striatum was sectioned coronally at 5 μm thickness to generate samples from 2mm rostral and 2mm caudal to the injection tract, and at the plane of the injection tract. Brain tissue sections were immunolabeled with the following antibodies: anti-HNA (Milipore, MAB1281), STEM121 (Takara, Y40410), anti-TH (Pel-Freez Biologicals, P40101), anti-Ki-67 (Abcam, Ab-15580), anti-5-HT (Immunostar, 20080). Tissue sections processed and stained for HNA/Ki-67 multiplex immunofluorescence were scanned to Whole Slide Images (WSI) with a Hamamatsu s60 slide scanner at 20x magnification and the digital images were imported into Visiopharm for automated image analysis. Cell index HNA/Ki-67 quantitative analysis was restricted to sections/areas where human cell grafts were manually identified by a trained scientist. An Analysis Protocol Package (APP) was developed in Visiopharm software to detect individual nuclei and classify/quantify HNA-positive and HNA/Ki-67-double positive cells present in each graft region. The Ki-67-positive cells were quantified as an index of the population of HNA-positive cells. Additional adjacent tissue sections were processed and stained for TH and 5-HT. The TH-positive cells were quantified as an index of the total population of cells. Quantitative analysis of TH-positive cells was restricted to sections/areas where human cell grafts were previously identified within HNA/Ki-67-stained tissue sections.

QUANTIFICATION AND STATISTICAL ANALYSIS

RNA-seq and WGS quality metrics were summarized using FastQC and samtools stats. Concordance and identity-match statistics were calculated using R v4.3.2. NeuriTest scoring pipelines were implemented in R v4.3.2 with custom scripts. PCA visualizations were generated with ggplot2 v3.5.2. No statistical adjustments for multiple testing were applied unless specified

Please cite this article in press as: Bratt-Leal et al., Genomic and transcriptomic quality control for an autologous iPSC-derived cell therapy for Parkinson's disease, Cell Stem Cell (2026), https://doi.org/10.1016/j.stem.2026.08.014

CellPress
OPEN ACCESS

Statistical Analysis

Statistical analysis was conducted on the data using IBM SPSS statistics software (v25). Repeated measures ANOVA were used to assess significance of data from rotation bias data (factors= Group [Intact control, Sham-transplant, 109, 111, 425, 457], Time [Pre-graft baseline, 4-, 8-, 12-, 16-, 20-, 24- and 28 weeks post-grafting]. Bonferroni's analysis was used as post-hoc analysis for all statistically significant ANOVA datasets. Group-wise comparisons using ANOVA was performed followed by Tukey's post-hoc analysis for fiber density in other brain regions. Statistical analysis for the GLP toxicology study was performed using GraphPad Prism. Group-wise comparisons using ANOVA was done followed by Dunnett's post-hoc analysis. All n values and what n represents are listed in the text and/or figure legends, and all p values obtained are listed in the figure legends. Blinding and randomization for the efficacy study were performed as described above.